

1 **Effects of elevated CO₂ and temperature on phytoplankton community**
2 **biomass, species composition and photosynthesis during an**
3 **experimentally induced autumn bloom in the Western English**
4 **Channel**

5 Matthew Keys^{1,2}, Gavin Tilstone^{1*}, Helen S. Findlay¹, Claire E. Widdicombe¹ and Tracy Lawson².

6 ¹ Plymouth Marine Laboratory, Prospect Place, The Hoe, Plymouth, PL1 3DH, UK.

7 ² University of Essex, Wivenhoe Park, Colchester, CO4 3SQ, UK.

8 *Correspondence to:* G. Tilstone (ghti@pml.ac.uk)

9

10 **Abstract**

11 The combined effects of elevated pCO₂ and temperature were investigated during an
12 experimentally induced autumn phytoplankton bloom *in vitro* sampled from the Western
13 English Channel (WEC). A full factorial 36-day microcosm experiment was conducted under
14 year 2100 predicted temperature (+ 4.5 °C) and pCO₂ levels (800 µatm). Over the experimental
15 period total phytoplankton biomass was significantly influenced by elevated pCO₂. At the end of
16 the experiment, biomass increased 6.5-fold under elevated pCO₂ and 4.6-fold under elevated
17 temperature relative to the ambient control. By contrast, the combined influence of elevated
18 pCO₂ and temperature had little effect on biomass relative to the control. Throughout the
19 experiment in all treatments and in the control, the phytoplankton community structure shifted
20 from dinoflagellates to nanophytoplankton . At the end of the experiment, under elevated pCO₂
21 nanophytoplankton contributed 90% of community biomass and was dominated by *Phaeocystis*
22 spp.. Under elevated temperature, nanophytoplankton comprised 85% of the community
23 biomass and was dominated by smaller nano-flagellates. In the control, larger nano-flagellates
24 dominated whilst the smallest nanophytoplankton contribution was observed under combined
25 elevated pCO₂ and temperature (~40 %). Under elevated pCO₂, temperature and in the control,
26 there was a significant decrease in dinoflagellate biomass. Under the combined effects of
27 elevated pCO₂ and temperature, dinoflagellate biomass increased and was dominated by the
28 harmful algal bloom (HAB) species, *Prorocentrum cordatum*. At the end of experiment,
29 Chlorophyll a (Chl *a*) normalised maximum photosynthetic rates (P^{B_m}) increased > 6-fold under
30 elevated pCO₂ and > 3-fold under elevated temperature while no effect on P^{B_m} was observed
31 when pCO₂ and temperature were elevated simultaneously. The results suggest that future
32 increases in temperature and pCO₂ simultaneously do not appear to influence coastal

33 phytoplankton productivity but significantly influence community composition during autumn
34 in the WEC.

35 **1. Introduction**

36 Oceanic concentration of CO₂ has increased by ~42% over pre-industrial levels, with a
37 continuing annual increase of ~0.4%. Current CO₂ level has reached ~400 µatm and has been
38 predicted to rise to >700 µatm by the end of this century (IPCC, 2013), with estimates exceeding
39 1000 µatm (Matear and Lenton, 2018; Raupach et al., 2007; Raven et al., 2005). With increasing
40 atmospheric CO₂, the oceans continue to absorb CO₂ from the atmosphere, which results in a
41 shift in oceanic carbonate chemistry resulting in a decrease in seawater pH or 'Ocean
42 Acidification' (OA). The projected increase in atmospheric CO₂ and corresponding increase in
43 ocean uptake, is predicted to result in a decrease in global mean surface seawater pH of 0.3
44 units below the present value of 8.1 to 7.8 (Wolf-gladrow et al., 1999). Under this scenario, the
45 shift in dissolved inorganic carbon (DIC) equilibria has wide ranging implications for
46 phytoplankton photosynthetic carbon fixation rates and growth (Riebesell, 2004).

47 Concurrent with OA, elevated atmospheric CO₂ and other climate active gases have warmed the
48 planet by ~0.6 °C over the past 100 years (IPCC, 2007). Atmospheric temperature has been
49 predicted to rise by a further 1.8 to 4 °C by the end of this century (Alley et al., 2007).

50 Phytoplankton metabolic activity may be accelerated by increased temperature (Eppley, 1972),
51 which can vary depending on the phytoplankton species and their physiological
52 requirements (Beardall. et al., 2009; Boyd et al., 2013). Long-term data sets already suggest that
53 ongoing changes in coastal phytoplankton communities are likely due to climate shifts and other
54 anthropogenic influences (Edwards et al., 2006; Smetacek and Cloern, 2008; Widdicombe et al.,
55 2010). The response to OA and temperature can potentially alter the community composition,
56 community biomass and photo-physiology. Understanding how these two factors may interact,
57 synergistically or antagonistically, is critical to our understanding and for predicting future
58 primary productivity (Boyd and Doney, 2002; Dunne, 2014).

59 Laboratory studies of phytoplankton species in culture and studies on natural populations in
60 the field have shown that most species exhibit sensitivity, in terms of growth and
61 photosynthetic rates, to elevated pCO₂ and temperature individually. To date, only a few studies
62 have investigated the interactive effects of these two parameters on natural populations (e.g.
63 Coello-Camba et al., 2014; Feng et al., 2009; Gao et al., 2017; Hare et al., 2007). Most laboratory
64 studies demonstrate variable results with species-specific responses. In the diatom
65 *Thalassiosira weissflogii* for example, pCO₂ elevated to 1000 µatm and + 5 °C temperature
66 synergistically enhanced growth, while the same conditions resulted in a reduction in growth

67 for the diatom *Dactyliosolen fragilissimus* (Taucher et al., 2015). Although there have been fewer
68 studies on dinoflagellates, variable responses have also been reported (Errera et al., 2014; Fu et
69 al., 2008). In natural populations, elevated pCO₂ has stimulated the growth of pico- and
70 nanophytoplankton (Boras et al., 2016; Engel et al., 2008) while increased temperature has
71 reduced their biomass (Moustaka-Gouni et al., 2016; Peter and Sommer, 2012). In a recent field
72 study on natural phytoplankton communities, elevated temperature (+ 3°C above ambient)
73 enhanced community biomass but the combined influence of elevated temperature and pCO₂
74 reduced the biomass (Gao et al., 2017).

75 Phytoplankton species composition, abundance and biomass has been measured since 1992 at
76 the time-series station L4 in the western English Channel (WEC), to evaluate how global
77 changes could drive future shifts in phytoplankton community structure and carbon
78 biogeochemistry. At this station, sea surface temperature and pCO₂ reach maximum values
79 during late summer and start to decline in autumn. During October, mean seawater
80 temperatures at 10 m decrease from 15.39 °C (± 0.49 sd) to 14.37 °C (± 0.62 sd). Following a
81 period of CO₂ oversaturation in late summer, pCO₂ returns to near-equilibrium at station L4 in
82 October when mean pCO₂ values decrease from 455.32 µatm (± 63.92 sd) to 404.06 µatm (±
83 38.55 sd) (Kitidis et al., 2012).

84 From a biological perspective, the autumn period at station L4 is characterised by the decline of
85 the late summer diatom and dinoflagellate blooms (Widdicombe et al., 2010) when their
86 biomass approaches values close to the time series minima (diatom biomass range: 6.01 (± 6.88
87 sd) – 2.85 (± 3.28 sd) mg C m⁻³; dinoflagellate biomass range: 1.75 (± 3.28 sd) – 0.66 (± 1.08 sd)
88 mg C m⁻³). Typically, over this period nanophytoplankton becomes numerically dominant and
89 biomass ranges from 20.94 (± 33.25 sd) – 9.38 (± 3.31 sd) mg C m⁻³, though there is
90 considerable variability in this biomass.

91 Based on the existing literature, the working hypotheses of this study are that: (1) community
92 biomass will increase differentially under individual treatments of elevated temperature and
93 pCO₂; (2) elevated pCO₂ will lead to taxonomic shifts due to differences in species-specific CO₂
94 concentrating mechanisms and/or RuBisCO specificity; (3) photosynthetic carbon fixation rates
95 will increase differentially under individual treatments of elevated temperature and pCO₂; (4)
96 elevated temperature will lead to taxonomic shifts due to species-specific thermal optima; (5)
97 temperature and pCO₂ elevated simultaneously will have synergistic effects.

98 The objective of the study was therefore to investigate the combined effects of elevated pCO₂
99 and temperature on phytoplankton community structure, biomass and photosynthetic carbon

100 fixation rates during the autumn transition from diatoms and dinoflagellates to
101 nanophytoplankton at station L4 in the WEC.

102 **2. Materials and methods**

103 **2.1 Perturbation experiment, sampling and experimental set-up**

104 Experimental seawater containing a natural phytoplankton community was sampled at station
105 L4 (50 ° 15' N, 4 ° 13' W) on 7th October 2015 from 10 m depth (40 L). The experimental
106 seawater was gently pre-filtered through a 200 µm Nitex mesh to remove mesozooplankton
107 grazers, into two 20 L acid-cleaned carboys. While grazers play an important role in regulating
108 phytoplankton community structure (e.g. Strom, 2002), our experimental goals considered only
109 the effects of elevated temperature and pCO₂, though the mesh size used does not remove
110 microzooplankton. In addition, 320 L of seawater was collected into sixteen 20 L acid-cleaned
111 carboys from the same depth for use as experimental media. Immediately upon return to the
112 laboratory the media seawater was filtered through an in-line 0.2 and 0.1 µm filter (Acropak™,
113 Pall Life Sciences) then stored in the dark at 14 °C until use. The experimental seawater was
114 gently and thoroughly mixed and transferred in equal parts from each carboy (to ensure
115 homogeneity) to sixteen 2.5 L borosilicate incubation bottles (4 sets of 4 replicates). The
116 remaining experimental seawater was sampled for initial (T0) concentrations of nutrients, Chl
117 *a*, total alkalinity, dissolved inorganic carbon, particulate organic carbon (POC) and nitrogen
118 (PON) and was also used to characterise the starting experimental phytoplankton community.
119 The incubation bottles were placed in an outdoor simulated in-situ incubation culture system
120 and each set of replicates was linked to one of four 22 L reservoirs filled with the filtered
121 seawater media. Neutral density spectrally corrected blue filters (Lee Filter no. 061) were
122 placed between polycarbonate sheets and mounted to the top, sides and ends of the incubation
123 system to provide ~50 % irradiance, approximating PAR measured at 10 m depth at station L4
124 on the day of sampling prior to starting experimental incubations (see **Fig. S1**, supplementary
125 material for time course of PAR levels during the experiment). The media was aerated with CO₂
126 free air and 5 % CO₂ in air precisely mixed using a mass flow controller (Bronkhorst UK
127 Limited) and used for the microcosm dilutions as per the following experimental design: (1)
128 control (390 µatm pCO₂, 14.5 °C matching station L4 in-situ values), (2) high temperature (390
129 µatm pCO₂, 18.5 °C), (3) high pCO₂ (800 µatm pCO₂, 14.5 °C) and (4) combination (800 µatm
130 pCO₂, 18.5 °C).

131 Initial nutrient concentrations (0.24 µM nitrate + nitrite, 0.086 µM phosphate and 2.14 µM
132 silicate on 7th October 2015) were amended to 8 µM nitrate+nitrite and 0.5 µM phosphate.
133 Pulses of nutrient inputs frequently occur at station L4 from August to December following

134 heavy rainfall events and subsequent riverine inputs to the system (e.g. Barnes et al., 2015). Our
135 nutrient amendments simulated these in situ conditions and were held constant to maintain
136 phytoplankton growth. Previous pilot studies highlighted that if these concentrations were not
137 maintained, the phytoplankton population crashes (Keys, 2017). As the phytoplankton
138 community was sampled over the transitional phase from diatoms and dinoflagellates to
139 nanophytoplankton, the in situ silicate concentration was maintained to reproduce the silicate
140 concentrations typical of this time of year (Smyth et al., 2010). Nutrient concentrations were
141 measured at time point T0 only.

142 Media transfer and sample acquisition was driven by peristaltic pumps. Following 48 hrs
143 acclimation in batch culture, semi-continuous daily dilution rates were maintained at between
144 10-13 % of the incubation bottle volume throughout the experiment. CO₂ enriched seawater
145 was added to the high CO₂ treatment replicates every 24 hrs, acclimating the natural
146 phytoplankton population to increments of elevated pCO₂ from ambient to ~800 µatm over 8
147 days followed by maintenance at ~800 µatm as per the method described by Schulz *et al*,
148 (2009). Adding CO₂ enriched seawater is the preferred protocol, since some phytoplankton
149 species are inhibited by the mechanical effects of direct bubbling (Riebesell et al., 2010; Shi et
150 al., 2009) which causes a reduction in growth rates and the formation of aggregates (Love et al.,
151 2016). pH was monitored daily to adjust the pCO₂ of the experimental media (+/-) prior to
152 dilutions to maintain target pCO₂ levels in the incubation bottles. The seasonality in pH and total
153 alkalinity (TA) are fairly stable at station L4 with high pH and low dissolved inorganic carbon
154 (DIC) during early summer, and low pH, high DIC throughout autumn and winter (Kitidis et al.,
155 2012). By maintaining the carbonate chemistry over the duration of the experiment, we aimed
156 to simulate natural events at the study site.

157 To provide sufficient time for changes in the phytoplankton community to occur and to achieve
158 an ecologically relevant data set, the incubation period was extended well beyond short-term
159 acclimation. Previous pilot studies using the same experimental protocols highlighted that after
160 ~20 days of incubation, significant changes in community structure and biomass were observed
161 (Keys, 2017). These results were used to inform a more relevant incubation period of 30+ days.

162 **2.2 Analytical methods, experimental seawater**

163 **2.2.1 Chlorophyll *a***

164 Chl *a* was measured in each incubation bottle. 100 mL triplicate samples from each replicate
165 were filtered onto 25 mm GF/F filters (nominal pore size 0.7 µm), extracted in 90 % acetone
166 overnight at -20 °C and Chl *a* concentration was measured on a Turner Trilogy™ fluorometer
167 using the non-acidified method of Welschmeyer (1994). The fluorometer was calibrated against

168 a stock Chl *a* standard (*Anacystis nidulans*, Sigma Aldrich, UK), the concentration of which was
169 determined with a Perkin Elmer™ spectrophotometer at wavelengths 663.89 and 750.11 nm.
170 Samples for Chl *a* analysis were taken every 2-3 days.

171 **2.2.2 Carbonate system**

172 70 mL samples for total alkalinity (TA) and dissolved inorganic carbon (DIC) analysis were
173 collected from each experimental replicate, stored in amber borosilicate bottles with no head
174 space and fixed with 40 µL of super-saturated Hg₂Cl₂ solution for later determination (Apollo
175 SciTech™ Alkalinity Titrator AS-ALK2; Apollo SciTech™ AS-C3 DIC analyser, with analytical
176 precision of 3 µmol kg⁻¹). Duplicate measurements were made for TA and triplicate
177 measurements for DIC. Carbonate system parameter values for media and treatment samples
178 were calculated from TA and DIC measurements using the programme CO₂sys (Pierrot et al.,
179 2006) with dissociation constants of carbonic acid of Mehrbach *et al.*, (1973) refitted by Dickson
180 and Millero (Dickson and Millero, 1987). Samples for TA and DIC were taken for analysis every
181 2-3 days throughout the experiment.

182 **2.2.3 Phytoplankton community analysis**

183 Phytoplankton community analysis was performed by flow cytometry (Becton Dickinson Accuri
184 ™ C6) for the 0.2 to 18 µm size fraction following Tarran *et al.*, (2006) and inverted light
185 microscopy was used to enumerate cells > 18 µm (BS EN 15204,2006). For flow cytometry, 2
186 mL samples fixed with glutaraldehyde to a final concentration of 2 % were flash frozen in liquid
187 nitrogen and stored at -80 °C for subsequent analysis. Phytoplankton data acquisition was
188 triggered on both chlorophyll fluorescence and forward light scatter (FSC) using prior
189 knowledge of the position of *Synechococcus* sp. to set the lower limit of analysis. Density plots of
190 FSC vs. CHL fluorescence, phycoerythrin fluorescence vs. CHL fluorescence and side scatter
191 (SSC) vs. CHL fluorescence were used to discriminate *Synechococcus* sp., picoeukaryote
192 phytoplankton (approx. 0.5–3 µm), coccolithophores, cryptophytes, *Phaeocystis* sp. single cells
193 and nanophytoplankton (eukaryotes >3 µm, excluding the coccolithophores, cryptophytes and
194 *Phaeocystis* sp. single cells), (for further information on flow cytometer calibration for
195 phytoplankton size measurements, see supplementary material). For inverted light microscopy,
196 140 mL samples were fixed with 2 % (final concentration) acid Lugol's iodine solution and
197 analysed by inverted light microscopy (Olympus™ IMT-2) using the Utermöhl counting
198 technique (Utermöhl, 1958; Widdicombe *et al.*, 2010). Phytoplankton community samples were
199 taken at T0, T10, T17, T24 and T36.

200 **2.2.4 Phytoplankton community biomass**

201 The smaller size fraction identified and enumerated through flow cytometry;
202 picophytoplankton, nanophytoplankton, *Synechococcus*, coccolithophores and cryptophytes
203 were converted to carbon biomass (mg C m^{-3}) using a spherical model to calculate mean cell
204 volume:

$$205 \left(\frac{4}{3} * \pi * r^3\right) \quad \text{Equation 1.}$$

206 and a conversion factor of $0.22 \text{ pg C } \mu\text{m}^{-3}$ (Booth, 1988). A conversion factor of $0.285 \text{ pg C } \mu\text{m}^{-3}$
207 was used for coccolithophores (Tarran et al., 2006) and cell a volume of $113 \mu\text{m}^3$ and carbon
208 cell⁻¹ value of 18 pg applied for *Phaeocystis* spp. (Widdicombe et al., 2010). *Phaeocystis* spp.
209 were identified and enumerated by flow cytometry separately to the nanophytoplankton class
210 due to high observed abundance in in the high pCO₂ treatment. Mean cell measurements of
211 individual species/taxa were used to calculate cell bio-volume for the $18 \mu\text{m} +$ size fraction
212 according to Kovalala and Larrance (1966) and converted to biomass according to the equations
213 of Menden-Deuer & Lessard, (2000).

214 **2.2.5 POC and PON**

215 Samples for particulate organic carbon (POC) and particulate organic nitrogen (PON) were
216 taken at T0, T15 and T36.150 mL samples were taken from each replicate and filtered under
217 gentle vacuum pressure onto pre-ashed 25mm glass fibre filters (GF/F, nominal pore size 0.7
218 μm). Filters were stored in acid washed petri-slides at $-20 \text{ }^\circ\text{C}$ until further processing. Sample
219 analysis was conducted using a Thermoquest Elemental Analyser (Flash 1112). Acetanilide
220 standards (Sigma Aldrich, UK) were used to calibrate measurements of carbon and nitrogen and
221 also used during the analysis to account for possible drift in measured concentrations.

222 **2.2.6 Chl fluorescence-based photophysiology**

223 Photosystem II (PSII) variable chlorophyll fluorescence parameters were measured using a fast
224 repetition rate fluorometer (FRRf) (FastOcean sensor in combination with an Act2Run
225 laboratory system, Chelsea Technologies, West Molesey, UK). The excitation wavelengths of the
226 FRRf's light emitting diodes (LEDs) were 450, 530 and 624 nm. The instrument was used in
227 single turnover mode with a saturation phase comprising 100 flashlets on a $2 \mu\text{s}$ pitch and a
228 relaxation phase comprising 40 flashlets on a $50 \mu\text{s}$ pitch. Measurements were conducted in a
229 temperature-controlled chamber at $15 \text{ }^\circ\text{C}$. The minimum (F_o) and maximum (F_m) Chl
230 fluorescence were estimated according to Kolber et al., (1998). Maximum quantum yields of PSII
231 were calculated as:

$$232 F_v / F_m = (F_m - F_o) / F_m \quad \text{Equation 2.}$$

233 PSII electron flux was calculated on a volume basis (JV_{PSII} ; $\text{mol e}^- \text{m}^{-3} \text{d}^{-1}$) using the absorption
 234 algorithm (Oxborough et al., 2012) following spectral correction by normalising the FRRf LED
 235 emission to the white spectra using Fast^{PRO} 8 software. This step required inputting the
 236 experimental phytoplankton community fluorescence excitation spectra values (FES). Since we
 237 did not measure the FES of our experimental samples, we used mean literature values for each
 238 phytoplankton group calculated proportionally (based on percentage contribution to total
 239 estimated biomass per phytoplankton group) as representative values for our experimental
 240 samples. The JV_{PSII} rates were converted to chlorophyll specific carbon fixation rates (mg C (mg
 241 $\text{Chl } a)^{-1} \text{m}^{-3} \text{h}^{-1}$), calculated as:

$$242 \quad JV_{PSII} \times \varphi_{E:C} \times MW_C / \text{Chl } a \quad \text{Equation 3}$$

243 where $\varphi_{E:C}$ is the electron requirement for carbon uptake ($\text{molecule CO}_2 \text{ (mol electrons)}^{-1}$), MW_C
 244 is the molecular weight of carbon and $\text{Chl } a$ is the $\text{Chl } a$ measurement specific to each sample.
 245 $\text{Chl } a$ specific JV_{PSII} based photosynthesis-irradiance curves were conducted in replicate batches
 246 between 10:00 – 16:00 to account for variability over the photo-period at between 8 - 14
 247 irradiance intensities. The maximum intensity applied was adjusted according to ambient
 248 natural irradiance on the day of sampling. Maximum photosynthetic rates of carbon fixation
 249 (P^B_m), the light limited slope (α^B) and the light saturation point of photosynthesis (I_k) were
 250 estimated by fitting the data to the model of Webb et al., (1974):

$$251 \quad P^B = (1 - e^{-\alpha \times I / P^B_m}) \quad \text{Equation 4}$$

252 Due to instrument failure during the experiment, samples for FRRf fluorescence-based light
 253 curves were taken at T36 only.

254 **2.3 Statistical analysis**

255 To test for effects of temperature, $p\text{CO}_2$ and possible time dependence of the measured response
 256 variables ($\text{Chl } a$, total biomass, POC, PON, photosynthetic parameters and biomass of individual
 257 species), generalized linear mixed models with the factors $p\text{CO}_2$, temperature and time (and all
 258 interactions) were applied to the data between T0 and T36. Analyses were conducted using the
 259 lme4 package in R (R Core Team (2014). R Foundation for Statistical Computing, Vienna,
 260 Austria).

261 **3. Results**

262 $\text{Chl } a$ concentration in the WEC at station L4 from 30 September - 6th October 2015 (when sea
 263 water was collected for the experiment) varied between 0.02-5 mg m^{-3} , with a mean
 264 concentration of $\sim 1.6 \text{ mg m}^{-3}$ (**Fig. 1 A**). Over the period leading up to phytoplankton
 265 community sampling, increasing nitrate and silicate concentrations coincided with a $\text{Chl } a$ peak

266 on 23rd September (**Fig. 1 B**). Routine net trawl (20 μm) sample observations indicated a
267 phytoplankton community dominated by the diatoms *Leptocylindrus danicus* and *L. minimus*
268 with a lower presence of the dinoflagellates *Prorocentrum cordatum*, *Heterocapsa* spp. and
269 *Oxytoxum gracile*. Following decreasing nitrate concentrations, there was a *P. cordatum* bloom
270 on 29th September, during the week before the experiment started (data not shown).

271 **3.1 Experimental carbonate system**

272 Equilibration to the target high pCO_2 values (800 μatm) within the high pCO_2 and combination
273 treatments was achieved at T10 (**Fig. 2 A & B**). These treatments were slowly acclimated to
274 increasing levels of pCO_2 over 7 days (from the initial dilution at T3) while the control and high
275 temperature treatments were acclimated at the same ambient carbonate system values as those
276 measured at station L4 on the day of sampling. Following equilibration, the mean pCO_2 values
277 within the control and high temperature treatments were 394.9 (± 4.3 sd) and 393.2 (± 4.8 sd)
278 μatm respectively, while in the high pCO_2 and combination treatments mean pCO_2 values were
279 822.6 (± 9.4) and 836.5 (± 15.6 sd) μatm , respectively. Carbonate system values remained stable
280 throughout the experiment (For full carbonate system measured and calculated parameters, see
281 **Table S1** in supplementary material).

282 **3.2 Experimental temperature treatments**

283 Mean temperatures in the control and high pCO_2 treatments were 14.1 (± 0.35 sd) $^\circ\text{C}$ and in the
284 high temperature and combination treatments the mean temperatures were 18.6 (± 0.42 sd) $^\circ\text{C}$,
285 with a mean temperature difference between the ambient and high temperature treatments of
286 4.46 (± 0.42 sd) $^\circ\text{C}$ (Supplementary material, **Fig. S2 A & B**).

287

288 **3.3 Chlorophyll *a***

289 Mean Chl *a* in the experimental seawater at T0 was 1.64 (± 0.02 sd) mg m^{-3} (**Fig. 3 A**). This
290 decreased in all treatments between T0 to T7, to ~ 0.1 (± 0.09 , 0.035 and 0.035 sd) mg m^{-3} in the
291 control, high pCO_2 and combination treatments, while in the high temperature treatment at T7
292 Chl *a* was 0.46 mg m^{-3} (± 0.29 sd) ($z = 2.176$, $p < 0.05$). From T7 to T12 Chl *a* increased in all
293 treatments which was highest in the combination (4.99 $\text{mg m}^{-3} \pm 0.69$ sd) and high pCO_2
294 treatments (3.83 $\text{mg m}^{-3} \pm 0.43$ sd). Overall, Chl *a* was significantly influenced by experimental
295 time, independent of experimental treatments (**Table 1**). At T36 Chl *a* concentration in the
296 combination treatment was higher (6.87 (± 0.58 sd) mg m^{-3}) than all other treatments while the
297 high temperature treatment concentration was higher (4.77 (± 0.44 sd) mg m^{-3}) than the control
298 and high pCO_2 treatment. Mean concentrations for the control and high pCO_2 treatment at T36

299 were not significantly different at $3.30 (\pm 0.22 \text{ sd})$ and $3.46 (\pm 0.35 \text{ sd}) \text{ mg m}^{-3}$ respectively
300 (pairwise comparison $t = 0.78, p = 0.858$).

301 **3.4 Phytoplankton biomass**

302 The starting biomass in all treatments was $110.2 (\pm 5.7 \text{ sd}) \text{ mg C m}^{-3}$ (**Fig. 3 B**). The biomass was
303 dominated by dinoflagellates ($\sim 50\%$) with smaller contributions from nanophytoplankton
304 ($\sim 13\%$), cryptophytes ($\sim 11\%$), diatoms ($\sim 9\%$), coccolithophores ($\sim 8\%$), *Synechococcus* ($\sim 6\%$)
305 and picophytoplankton ($\sim 3\%$). Total biomass was significantly influenced in all treatments over
306 time (**Table 1**) and at T10, it was significantly higher in the high temperature treatment when
307 biomass reached $752 (\pm 106 \text{ sd}) \text{ mg C m}^{-3}$ ($z = 2.769, p < 0.01$). Biomass was significantly higher
308 in the elevated pCO₂ treatment (interaction of time x high pCO₂) (**Table 1**), reaching $2481 (\pm$
309 $182.68 \text{ sd}) \text{ mg C m}^{-3}$ at T36, ~ 6.5 -fold higher than the control ($z = 3.657, p < 0.001$). Total
310 biomass in the high temperature treatment at T36 was significantly higher than the
311 combination treatment and ambient control ($z = 2.744, p < 0.001$), which were $525 (\pm 28.02 \text{ sd})$
312 mg C m^{-3} and $378 (\pm 33.95 \text{ sd}) \text{ mg C m}^{-3}$, respectively. Reaching $1735 (\pm 169.24 \text{ sd}) \text{ mg C m}^{-3}$,
313 biomass in the high temperature treatment was ~ 4.6 -fold higher than the control.

314 POC followed the same trends in all treatments between T0 and T36 (**Fig. 3 C**) and was in close
315 range of the estimated biomass ($R^2 = 0.914$, **Fig. 3 D**). POC was significantly influenced by the
316 interaction of time x high pCO₂ and time x high temperature (**Table 1**). At T36 POC was
317 significantly higher in the high pCO₂ treatment ($2086 \pm 155.19 \text{ sd mg m}^{-3}$) followed by the high
318 temperature treatment ($1594 \pm 162.24 \text{ sd mg m}^{-3}$), ~ 5.4 -fold and 4-fold higher than the control,
319 respectively. whereas a decline in POC was observed in the control and combination treatment.
320 PON followed the same trend as POC over the course of the experiment, though it was only
321 significantly influenced by the interaction between time x high pCO₂ (**Fig. 3 E, Table 1**). At T36
322 concentrations were $147 (\pm 12.99 \text{ sd})$ and $133 (\pm 15.59 \text{ sd}) \text{ mg m}^{-3}$ in the high pCO₂ and high
323 temperature treatments respectively, while PON was $57.75 (\pm 13.07 \text{ sd}) \text{ mg m}^{-3}$ in the
324 combination treatment and $47.18 (\pm 9.32 \text{ sd}) \text{ mg m}^{-3}$ in the control. POC:PON ratios were
325 significantly influenced by the interaction of time x high pCO₂ and time x high temperature
326 (**Table 1**). The largest increase of 33 %, from 10.72 to $14.26 (\pm 1.73 \text{ sd}) \text{ molC:molN}$ was in the
327 high pCO₂ treatment (73% higher than the control), followed by an increase of 32 % to $9.83 (\pm$
328 $1.82 \text{ sd}) \text{ molC:molN}$ in the combination treatment (19% higher than the control), and an
329 increase of 17 % to $12.09 (\pm 2.14 \text{ sd}) \text{ molC:molN}$ in the high temperature treatment (46%
330 higher than the control). In contrast, the POC:PON ratio in the control declined by 20 % from T0
331 to T36, from 10.33 to $8.26 (\pm 0.50 \text{ sd}) \text{ molC:molN}$ (**Fig. 3 F**).

332

333 3.5 Community composition

334 From T0 to T24 the community shifted away from dominance of dinoflagellates in all
335 treatments, followed by further regime shifts between T24 and T36 in the control and
336 combination treatments. At T36 diatoms dominated the phytoplankton community biomass in
337 the ambient control (**Fig. 4 A**), while the high temperature and high pCO₂ treatments exhibited
338 near mono-specific dominance of nanophytoplankton (**Figs. 4 B & C**). The most diverse
339 community was in the combination treatment where dinoflagellates and *Synechococcus* became
340 more prominent (**Fig. 4 D**).

341 Between T10 and T24 the community shifted to nanophytoplankton in all experimental
342 treatments. This dominance was maintained to T36 in the high temperature and high pCO₂
343 treatments whereas in the ambient control and combination treatment, the community shifted
344 away from nanophytoplankton (**Fig. 5 A**). Nanophytoplankton biomass was significantly higher
345 in the high pCO₂ treatment (**Table 2**) with biomass reaching 2216 (± 189.67 sd) mg C m⁻³ at
346 T36. This biomass was also high (though not significantly throughout the experiment until T36)
347 in the high temperature treatment (T36: 1489 (± 170.32 sd) mg C m⁻³, $z = 1.695$, $p = 0.09$)
348 compared to the control and combination treatments. In the combination treatment
349 nanophytoplankton biomass was 238 (± 14.16 sd) mg C m⁻³ at T36 which was higher than the
350 control, though not significantly (162 ± 20.02 sd mg C m⁻³). In addition to significant differences
351 in nanophytoplankton biomass amongst the experimental treatments, treatment-specific
352 differences in cell size were also observed. Larger nano-flagellates dominated the control (mean
353 cell diameter of 6.34 μ m), smaller nano-flagellates dominated the high temperature and
354 combination treatments (mean cell diameters of 3.61 μ m and 4.28 μ m) whereas *Phaeocystis* spp.
355 dominated the high pCO₂ treatment (mean cell diameter 5.04 μ m) and was not observed in any
356 other treatment (Supplementary material, **Fig. S3 A-D**).

357 At T0, diatom biomass was low and dominated by *Coscinodiscus wailessi* (48 %; 4.99 mg C m⁻³),
358 *Pleurosigma* (25 %; 2.56 mg C m⁻³) and *Thalassiosira subtilis* (19 %; 1.94 mg C m⁻³). Small
359 biomass contributions were made by *Navicula distans*, undetermined pennate diatoms and
360 *Cylindrotheca closterium*. Biomass in the diatom group remained low from T0 to T24 but
361 increased significantly through time in all treatments (**Table 2**), with the highest biomass in the
362 high pCO₂ treatment (235 ± 21.41 sd mg C m⁻³, **Fig. 5 B**). The highest diatom contribution to
363 total community biomass at T36 was in the ambient control (52 % of biomass; 198 ± 17.28 sd
364 mg C m⁻³). In both the high temperature and combination treatments diatom biomass was lower
365 at T36 (151 ± 10.94 sd and 124 ± 19.16 sd mg C m⁻³, respectively). In all treatments, diatom
366 biomass shifted from the larger *C. wailessi* to the smaller *C. closterium*, *N. distans*, *T. subtilis* and
367 *Tropidoneis* spp., the relative contributions of which were treatment-specific. Overall *N. distans*

368 dominated diatom biomass in all treatments at T36 (ambient control: 112 ± 24.86 sd mg C m⁻³,
369 56 % of biomass; high temperature: 106 ± 17.75 sd mg C m⁻³, 70 % of biomass; high pCO₂: $152 \pm$
370 19.09 sd mg C m⁻³, 61 % of biomass; and combination: 111 ± 20.97 sd mg C m⁻³, 89 % of
371 biomass; Supplementary material, **Fig. S4 A-D**).

372 The starting dinoflagellate community was dominated by *Gyrodinium spirale* (91 %; 49 mg C m⁻³,
373 ³), with smaller contributions from *Katodinium glaucum* (5 %; 2.76 mg C m⁻³), *Prorocentrum*
374 *cordatum* (3 %; 1.78 mg C m⁻³) and undetermined *Gymnodiniales* (1 %; 0.49 mg C m⁻³). At T36
375 Dinoflagellate biomass was significantly higher in the combination treatment (90 ± 16.98 sd mg
376 C m⁻³, **Fig. 5 C, Table 2**) followed by the high temperature treatment (57 ± 6.87 sd mg C m⁻³,
377 **Table 2**). There was no significant difference in dinoflagellate biomass between the high pCO₂
378 treatment and ambient control at T36 when biomass was low. In the combination treatment, the
379 dinoflagellate biomass became dominated by *P. cordatum* which contributed 59 ± 12.95 sd mg C
380 m⁻³ (66 % of biomass in this group).

381 *Synechococcus* biomass was significantly higher in the combination treatment (reaching $59.9 \pm$
382 4.30 sd mg C m⁻³ at T36, **Fig. 5 D, Table 2**) followed by the high temperature treatment ($30 \pm$
383 5.98 sd mg C m⁻³, **Table 2**). In both the high pCO₂ treatment and control *Synechococcus* biomass
384 was low (~ 7 mg C m⁻³ in both treatments at T36), though an initial significant response to high
385 pCO₂ was observed between T0 – T10 (**Table 2**). In all treatments and throughout the
386 experiment, relative to the other phytoplankton groups, biomass of picophytoplankton (**Fig. 5**
387 **E**), cryptophytes (**Fig. 5 F**) and coccolithophores (**Fig. 5 G**) remained low, though there was a
388 slight increase in picophytoplankton in the combination treatment (11.26 ± 0.79 sd mg C m⁻³;
389 **Table 2**).

390 Microzooplankton was dominated by *Strombolidium* spp. in all treatments throughout the
391 experiment, though biomass was low relative to the phytoplankton community (**Fig. 6**).
392 Following a decline from T0 to T10, microzooplankton biomass increased in all but the high CO₂
393 treatment until T17 when biomass diverged. The biomass trajectory maintained an increase in
394 the control when at T36 it was highest at ~ 1.6 mg C m⁻³, 90% higher than the high temperature
395 treatment (0.83 mg C m⁻³). Microzooplankton biomass was significantly lower in the high CO₂
396 treatment at T36 ($z = -2.100$, $p = 0.036$) and undetected in the combination treatment at this
397 time point (**Table 2**).

398

399 **3.6 Chl *a* fluorescence-based photophysiology**

400 At T36, FRRf photosynthesis-irradiance (PE) parameters were strongly influenced by the
401 experimental treatments. P^B_m was significantly higher in the high pCO₂ treatment (18.93 mg C
402 (mg Chl *a*)⁻¹ m⁻³ h⁻¹), followed by the high temperature treatment (9.58 mg C (mg Chl *a*)⁻¹ m⁻³ h⁻¹;
403 **Fig. 7, Tables 3 & 4**). There was no significant difference in P^B_m between the control and
404 combination treatments (2.77 and 3.02 mg C (mg Chl *a*)⁻¹ m⁻³ h⁻¹). Light limited photosynthetic
405 efficiency (α^B) also followed the same trend and was significantly higher in the high pCO₂
406 treatment (0.13 mg C (mg Chl *a*)⁻¹ m⁻³ h⁻¹ ($\mu\text{mol photon m}^{-2} \text{s}^{-1}$)⁻¹) followed by the high
407 temperature treatment (0.09 mg C (mg Chl *a*)⁻¹ m⁻³ h⁻¹ ($\mu\text{mol photon m}^{-2} \text{s}^{-1}$)⁻¹; **Tables 3 & 4**). α^B
408 was low in both the control and combination treatment (0.03 and 0.04 mg C (mg Chl *a*)⁻¹ m⁻³ h⁻¹
409 ($\mu\text{mol photon m}^{-2} \text{s}^{-1}$)⁻¹, respectively). The light saturation point of photosynthesis (E_k) was
410 significantly higher in the high pCO₂ treatment relative to all treatments (144.13 $\mu\text{mol photon}$
411 $\text{m}^{-2} \text{s}^{-1}$), though significantly lower in the combination treatment relative to both the high pCO₂
412 and high temperature treatments (**Tables 3 & 4**).

413 **4. Discussion**

414 Individually, elevated temperature and pCO₂ resulted in the highest biomass and maximum
415 photosynthetic rates (P^B_m) at T36, when nanophytoplankton dominated. The interaction of
416 these two factors had little effect on total biomass with values close to the ambient control, and
417 no effect on P^B_m . The combination treatment, however, exhibited the greatest diversity of
418 phytoplankton functional groups with dinoflagellates and *Synechococcus* becoming dominant
419 over time.

420 Elevated pCO₂ has been shown to enhance the growth and photosynthesis of some
421 phytoplankton species which have active uptake systems for inorganic carbon (Giordano et al.,
422 2005; Reinfelder, 2011). Elevated pCO₂ may therefore lead to lowered energetic costs of carbon
423 assimilation in some species and a redistribution of the cellular energy budget to other
424 processes (Tortell et al., 2002). In this study, under elevated pCO₂ where the dominant group
425 was nanophytoplankton, the most abundant species was the haptophyte *Phaeocystis* spp.
426 Photosynthetic carbon fixation in *Phaeocystis* spp. is presently near saturation with respect to
427 current levels of pCO₂ (Rost et al., 2003). Dominance of this spp. under elevated pCO₂ may be
428 due to lowered grazing pressure since microzooplankton biomass was lowest in the high CO₂
429 treatment throughout the experiment. The increased biomass and photosynthetic carbon
430 fixation in this experimental community under elevated pCO₂ is due to the community shift to
431 *Phaeocystis* spp.. The increased biomass in the high temperature treatment (where
432 microzooplankton biomass remained stable between T17 to T36, though lower than the
433 control) may be attributed to enhanced enzymatic activities, since algal growth commonly
434 increases with temperature until after an optimal range (Boyd et al., 2013; Goldman and

435 Carpenter, 1974; Savage et al., 2004). Optimum growth temperatures for marine phytoplankton
436 are often several degrees higher than environmental temperatures (Eppley, 1972; Thomas et al.,
437 2012). Nanophytoplankton also dominated in this treatment and while *Phaeocystis* spp. was not
438 discriminated, no further classification was made at a group/species level. Reduced biomass in
439 the control from T24 onwards may be due to increased grazing pressure given the highest
440 concentrations of microzooplankton biomass were observed in the control. Conversely,
441 microzooplankton biomass declined significantly from T17 in the combination treatment,
442 indicating reduced grazing pressure while phytoplankton biomass also declined from this time
443 point. Nutrient concentrations were not measured beyond T0 and we cannot therefore exclude
444 the possibility that differences in nutrient availability may have contributed to observed
445 differences between control and high temperature and high CO₂ treatments.

446 **4.1 Chl *a***

447 Biomass in the control peaked at T25 followed by a decline to T36. Correlated with this, Chl *a*
448 also peaked at T25 in the control and declined to 3.3 mg m⁻³ by T27, remaining close to this
449 value until T36. Biomass in the combination treatment peaked at T20 followed by decline to
450 T36 whereas Chl *a* in this treatment declined from T20 to T25 followed by an increase at T27
451 before further decline similar to the biomass. Chl *a* peaked in this treatment again at T36 (6.8
452 mg m⁻³). We attribute the increase in Chl *a* between T25 – T27 (coincident with an overall
453 biomass decrease) to lower species specific carbon:Chl *a* ratios as a result of the increase in
454 dinoflagellates, *Synechococcus* and picophytoplankton biomass from T25. We speculate that the
455 decline in biomass under nutrient replete conditions in the combination treatment was
456 probably due to slower species-specific growth rates when diatoms and dinoflagellates became
457 more prominent in this treatment. Carbon:Chl *a* in diatoms and dinoflagellates have previously
458 been demonstrated to be lower than nano- and picophytoplankton (Sathyendranath et al.,
459 2009) This contrasts the results reported in comparable studies as Chl *a* is generally highly
460 correlated with biomass, (e.g. Feng et al., 2009). Similar results were reported however by Hare
461 et al., (2007) which indicates that Chl *a* may not always be a reliable proxy for biomass in mixed
462 communities.

463 **4.2 Biomass**

464 This study shows that the phytoplankton community response to elevated temperature and
465 pCO₂ is highly variable. pCO₂ elevated to ~800 µatm induced higher community biomass, similar
466 to the findings of Kim et al., (2006), whereas in other natural community studies no CO₂ effect
467 on biomass was observed (Delille et al., 2005; Maugendre et al., 2017; Paul et al., 2015). A ~4.5
468 °C increase in temperature also resulted in higher biomass at T36 in this study, similar to the

469 findings of Feng et al., (2009) and Hare et al., (2007) though elevated temperature has
470 previously reduced biomass of natural nanophytoplankton communities in the Western Baltic
471 Sea and Arctic Ocean (Coello-Camba et al., 2014; Moustaka-Gouni et al., 2016). When elevated
472 temperature and pCO₂ were combined, community biomass exhibited little response, similar to
473 the findings of Gao et al., (2017), though an increase in biomass has also been reported (Calbet
474 et al., 2014; Feng et al., 2009). Geographic location and season also play an important role in
475 structuring the community and its response in terms of biomass to elevated temperature and
476 pCO₂. (Li et al., 2009; Morán et al., 2010). This may explain part of the variability in responses
477 observed from studies on phytoplankton during different seasons and provinces.

478 **4.3 Carbon:Nitrogen**

479 In agreement with others, the results of this experiment showed highest increases in C:N under
480 elevated pCO₂ alone (Riebesell et al., 2007). C:N also increased under high temperature,
481 consistent with the findings of Lomas and Glibert, (1999) and Taucher et al., (2015). It also
482 increased when pCO₂ and temperature were elevated, albeit to a lesser degree, which was also
483 observed by Calbet et al., (2014), but contrasts other studies that have observed C:N being
484 unaffected by the combined influence of elevated pCO₂ and temperature (Deppeler and
485 Davidson, 2017; Kim et al., 2006; C. Paul et al., 2015). C:N is a strong indicator of cellular protein
486 content (Woods and Harrison, 2003) and increases under elevated pCO₂ and warming may lead
487 to lowered nutritional value of phytoplankton which has implications for zooplankton
488 reproduction and the biogeochemical cycling of nutrients.

489 **4.4 Photosynthetic carbon fixation rates**

490 At T36, under elevated pCO₂ P^B_m was > 6 times higher than in the control, but only one time
491 point was measured so we are not able to make decisive conclusions. Riebesell et al., (2007) and
492 Tortell et al., (2008) also reported an increase in P^B_m under elevated pCO₂. By contrast other
493 observations on natural populations under elevated pCO₂ reported a reduction in P^B_m (Feng et
494 al., 2009; Hare et al., 2007). Studies on laboratory cultures have shown that increases in
495 temperature cause an increase photosynthetic rates (Feng et al., 2008; Fu et al., 2007; Hutchins
496 et al., 2007), similar to what we observed in this study. In the combined pCO₂ and temperature
497 treatment, we found no effect on P^B_m, which has also been observed in experiments on natural
498 populations (Coello-Camba and Agustí, 2016; Gao et al., 2017). This contrasts the findings of
499 Feng et al., (2009) and Hare et al., (2007) who observed the highest P^B_m when temperature and
500 pCO₂ were elevated simultaneously. In this study, increases in α^B and E_k under elevated pCO₂,
501 and a decrease in these parameters when elevated pCO₂ and temperature were combined also
502 contrasts the trends reported by Feng et al., (2009). We should stress however, that while our

503 photophysiological measurements support our observed trends in community biomass, they
504 were made on a single occasion at the end of the experiment. Future experiments should focus
505 on acquiring photophysiological measurements throughout.

506 Species specific photosynthetic rates have been demonstrated to decrease beyond their thermal
507 optimum (Raven and Geider, 1988) which can be modified through photoprotective rather than
508 photosynthetic pigments (Kiefer and Mitchell, 1983). This may explain the difference in P^B_m
509 between the high pCO_2 and high temperature treatments (in addition to differences in
510 nanophytoplankton community composition in relation to *Phaeocystis* spp. discussed above), as
511 the experimental high temperature treatment in this study was ~ 4.5 ° C higher than the control.

512 There was no significant effect of combined elevated pCO_2 and temperature on P^B_m , which was
513 strongly influenced by taxonomic differences between the experimental treatments. Warming
514 has been shown to lead to smaller cell sizes in nanophytoplankton (Atkinson et al., 2003; Peter
515 and Sommer, 2012), which was observed in the combined treatment together with decreased
516 nanophytoplankton biomass. Diatoms also shifted to smaller species with reduced biomass,
517 while dinoflagellate and *Synechococcus* biomass increased at T36. Dinoflagellates are the only
518 photoautotrophs with form II RuBisCO (Morse et al., 1995) which has the lowest
519 carboxylation:oxygation specificity factor among eukaryotic phytoplankton (Badger et al.,
520 1998), which may give dinoflagellates a disadvantage in carbon fixation under present ambient
521 pCO_2 levels. Phytoplankton growth rates are generally slower in surface waters with high pH
522 (≥ 9) resulting from photosynthetic removal of CO_2 by previous blooms and the associated
523 nutrient depletion (Hansen, 2002; Hinga, 2002). Though growth under high pH provides
524 indirect evidence that dinoflagellates possess CCMs, direct evidence is limited and points to the
525 efficiency of CCMs in dinoflagellates as moderate in comparison to diatoms and some
526 haptophytes (Reinfelder, 2011 and references therein). Given that dinoflagellates accounted for
527 just $\sim 20\%$ of biomass in the combination treatment, exerting a minor influence on community
528 photosynthetic rates, further work is required to explain the lower P^B_m under the combined
529 influence of elevated pCO_2 and temperature compared to the individual treatment influences.
530 We applied the same electron requirement parameter for carbon uptake across all treatments,
531 though in nature and between species, there can be considerable variation in this parameter
532 (e.g. 1.15 to 54.2 mol e^- (mol C) $^{-1}$; Lawrenz et al., 2013) which can co-vary with temperature,
533 nutrients, Chl *a*, irradiance and community structure. Better measurement techniques at
534 quantifying this variability are necessary in the future.

535 **4.5 Community composition**

536 Phytoplankton community structure changes were observed, with a shift from dinoflagellates to
537 nanophytoplankton which was most pronounced under single treatments of elevated
538 temperature and pCO₂. Amongst the nanophytoplankton, a distinct size shift to smaller cells was
539 observed in the high temperature and combination treatments, while in the high pCO₂
540 treatment *Phaeocystis* spp. dominated. Under combined pCO₂ and temperature from T24
541 onwards however, dinoflagellate and *Synechococcus* biomass increased and nanophytoplankton
542 biomass decreased. An increase in pico- and nanophytoplankton has previously been reported
543 in natural communities under elevated pCO₂ (Bermúdez et al., 2016; Boras et al., 2016;
544 Brussaard et al., 2013; Engel et al., 2008) while no effect on these size classes has been observed
545 in other studies (Calbet et al., 2014; Paulino et al., 2007). Moustaka-Gouni et al., (2016) also
546 found no CO₂ effect on natural nanophytoplankton communities but increased temperature
547 reduced the biomass of this group. Kim et al., (2006) observed a shift from nanophytoplankton
548 to diatoms under elevated pCO₂ alone while a shift from diatoms to nanophytoplankton under
549 combined elevated pCO₂ and temperature has been reported (Hare et al., 2007). A variable
550 response in *Phaeocystis* spp. to elevated pCO₂ has also been reported with increased growth
551 (Chen et al., 2014; Keys et al., 2017), no effect (Thoisen et al., 2015) and decreased growth
552 (Hoogstraten et al., 2012) observed. *Phaeocystis* spp. can outcompete other phytoplankton and
553 form massive blooms (up to 10 g C m⁻³) with impacts on food webs, global biogeochemical
554 cycles and climate regulation (Schoemann et al., 2005). While not a toxic algal species,
555 *Phaeocystis* spp. are considered a harmful algal bloom (HAB) species when biomass reaches
556 sufficient concentrations to cause anoxia through the production of mucus foam which can clog
557 the feeding apparatus of zooplankton and fish (Eilertsen & Raa, 1995).

558 Recently published studies on the response of diatoms to elevated pCO₂ and temperature vary
559 greatly. For example, Taucher et al., (2015) showed that *Thalassiosira weissflogii* incubated at
560 1000 µatm pCO₂ increased growth by 8 % while for *Dactyliosolen fragilissimus*, growth
561 increased by 39 %; temperature elevated by + 5°C also had a stimulating effect on *T. weissflogii*
562 but inhibited the growth rate of *D. fragilissimus*; and when the treatments were combined
563 growth was enhanced in *T. weissflogii* but reduced in *D. fragilissimus*. In our study, elevated pCO₂
564 increased biomass in diatoms (time dependent), but elevated temperature and the combination
565 of these factors reduced the signal of this response. A distinct size-shift in diatom species was
566 observed in all treatments, from the larger *Coscinodiscus* spp., *Pleurosigma* and *Thalassiosira*
567 *subtilis* to the smaller *Navicula distans*. This was most pronounced in the combination treatment
568 where *N. distans* formed 89 % of diatom biomass. *Navicula* spp. previously exhibited a
569 differential response to both elevated temperature and pCO₂. At + 4.5 °C and 960 ppm CO₂
570 Torstensson et al., (2012) observed no synergistic effects on the benthic *Navicula directa*.

571 Elevated temperature increased growth rates by 43 % while a reduction of 5 % was observed
572 under elevated CO₂. No effects on growth were detected at pH ranging from 8 – 7.4 units in
573 *Navicula* spp. (Thoisen et al., 2015), while there was a significant increase in growth in *N.*
574 *distans* along a CO₂ gradient at a shallow cold-water vent system (Baragi et al., 2015).

575 *Synechococcus* grown under pCO₂ elevated to 750 ppm and temperature elevated by 4 °C
576 resulted in increased growth and a 4-fold increase in P^{B_m} (Fu et al., 2007) which is similar to the
577 results of the present study.

578 The combination of elevated temperature and pCO₂ significantly increased dinoflagellate
579 biomass to 17 % of total biomass. This was due to *P. cordatum* which increased biomass by
580 more than 30-fold from T0 to T30 (66 % of dinoflagellate biomass in this treatment). Despite
581 the global increase in the frequency of HABs few studies have focussed on the response of
582 dinoflagellates to elevated pCO₂ and temperature. In laboratory studies at 1000 ppm CO₂,
583 growth rates of the HAB species *Karenia brevis* increased by 46 %, at 1000 ppm CO₂ and + 5 °C
584 temperature it's growth increased by 30 % but was reduced under elevated temperature alone
585 (Errera et al., 2014). A combined increase in pCO₂ and temperature enhanced both the growth
586 and P^{B_m} in the dinoflagellate *Heterosigma akashiwo*, whereas in contrast to the present findings,
587 only pCO₂ alone enhanced these parameters in *P. cordatum* (Fu et al., 2008).

588 **5. Implications**

589 Increased biomass, P^{B_m} and a community shift to nanophytoplankton under individual increases
590 in temperature and pCO₂ suggests a potential negative feedback on atmospheric CO₂, whereby
591 more CO₂ is removed from the ocean, and hence from the atmosphere through an increase in
592 photosynthesis. The selection of *Phaeocystis* spp. under elevated pCO₂ indicates the potential for
593 negative impacts on ecosystem function and food web structure due to the formation of hypoxic
594 zones which can occur under eutrophication, inhibitory feeding effects and lowered fecundity in
595 many copepods associated with this species (Schoemann et al., 2005; Verity et al., 2007). While
596 more CO₂ is fixed, selection for nanophytoplankton in both of these treatments however, may
597 result in reduced carbon sequestration due to slower sinking rates of the smaller phytoplankton
598 cells (Bopp et al., 2001; Laws et al., 2000). When temperature and pCO₂ were elevated
599 simultaneously, community biomass showed little response and no effects on P^{B_m} were
600 observed. This suggests no change on feedback to atmospheric CO₂ and climate warming in
601 future warmer high CO₂ oceans. Additionally, combined elevated pCO₂ and temperature
602 significantly modified taxonomic composition, by reducing diatom biomass relative to the
603 control with an increase in dinoflagellate biomass dominated by the HAB species, *P. cordatum*.
604 This has implications for fisheries, ecosystem function and human health.

605 **6. Conclusion**

606 These experimental results provide new evidence that increases in pCO₂ coupled with rising sea
607 temperatures may have antagonistic effects on the autumn phytoplankton community in the
608 WEC. Under future global change scenarios, the size range and biomass of diatoms may be
609 reduced with increased dinoflagellate biomass and the selection of HAB species. The
610 experimental simulations of year 2100 temperature and pCO₂ demonstrate that the effects of
611 warming can be offset by elevated pCO₂, maintaining current levels of coastal phytoplankton
612 productivity while significantly altering the community structure, and in turn these shifts will
613 have consequences on carbon biogeochemical cycling in the WEC.

614 **Data availability:** Experimental data used for analysis will be made available (DOI will be
615 created)

616 **Author contributions:** Matthew Keys collected, measured, processed and analysed the data and
617 prepared the figures. Drs Gavin Tilstone and Helen Findlay conceived, directed and sought the
618 necessary funds to support the research. Matthew Keys and Dr Gavin Tilstone wrote the paper
619 with input from Claire Widdicombe and Professor Tracy Lawson. Claire Widdicombe supervised
620 and advised on phytoplankton taxonomic classifications.

621 **Competing interests:** The authors declare that they have no conflict of interest.

622 **Acknowledgements:** G.H.T, H.S.F. and C.E.W were supported by the UK Natural Environment
623 Research Council's (NERC) National Capability – The Western English Channel Observatory
624 (WCO). C.E.W was also partly funded by the NERC and Department for Environment, Food and
625 Rural Affairs, Marine Ecosystems Research Program (Grant no. NE/L003279/1). M.K. was
626 supported by a NERC PhD studentship (grant No. NE/L50189X/1). We thank Glen Tarran for his
627 training, help and assistance with flow cytometry, The National Earth Observation Data Archive
628 and Analysis Service UK (NEODAAS) for providing the MODIS image used in Fig 1. and the crew
629 of RV Plymouth Quest for their helpful assistance during field sampling.

630 **References**

631 Alley, D., Berntsen, T., Bindoff, N. L., Chen, Z. L., Chidthaisong, A., Friedlingstein, P., Gregory, J., G.,
632 H., Heimann, M., Hewitson, B., Hoskins, B., Joos, F., Jouzel, J., Kattsov, V., Lohmann, U., Manning, M.,
633 Matsuno, T., Molina, M., Nicholls, N., Overpeck, J., Qin, D.H., Raga, G., Ramaswamy, V., Ren, J.W.,
634 Rusticucci, M., Solomon, S. and Somerville, R., Stocker, T.F., Stott, P., Stouffer, R.J. Whetton, P.,
635 Wood, R.A. & Wratt, D.: Climate Change 2007. The Physical Science basis: Summary for

636 policymakers. Contribution of Working Group I to the Fourth Assessment Report of the
637 Intergovernmental Panel on Climate Change, in ... Climate Change 2007. The Physical Science
638 Basis, Summary for Policy Makers.... [online] Available from:
639 <http://scholar.google.com/scholar?hl=en&btnG=Search&q=intitle:Climate+Change+2007+:+The+Physical+Science+Basis+Summary+for+Policymakers+Contribution+of+Working+Group+I+to+the+Fourth+Assessment+Report+of+the#3> (Accessed 24 October 2013), 2007.

642 Atkinson, D., Ciotti, B. J. and Montagnes, D. J. S.: Protists decrease in size linearly with
643 temperature: ca. 2.5% C⁻¹, Proc. R. Soc. B Biol. Sci., 270(1533), 2605–2611,
644 doi:10.1098/rspb.2003.2538, 2003.

645 Badger, M. R., Andrews, T. J., Whitney, S. M., Ludwig, M., Yellowlees, D. C., Leggat, W. and Price, G.
646 D.: The diversity and coevolution of Rubisco , plastids , pyrenoids , and chloroplast-based CO₂ -
647 concentrating mechanisms in algae 1, Can. J. Bot., (76), 1052–1071, 1998.

648 Baragi, L. V., Khandeparker, L. and Anil, A. C.: Influence of elevated temperature and pCO₂ on the
649 marine periphytic diatom *Navicula distans* and its associated organisms in culture,
650 *Hydrobiologia*, 762(1), 127–142, doi:10.1007/s10750-015-2343-9, 2015.

651 Barnes, M. K., Tilstone, G. H., Smyth, T. J., Widdicombe, C. E., Gloël, J., Robinson, C., Kaiser, J. and
652 Suggett, D. J.: Drivers and effects of *Karenia mikimotoi* blooms in the western English Channel,
653 *Prog. Oceanogr.*, 137, 456–469, doi:10.1016/j.pocean.2015.04.018, 2015.

654 Beardall, J., Stojkovic, S. and Larsen, S.: Living in a high CO₂ world: impacts of global climate
655 change on marine phytoplankton, *Plant Ecol. Divers.*, 2(2), 191–205,
656 doi:10.1080/17550870903271363, 2009.

657 Bermúdez, J. R., Riebesell, U., Larsen, A. and Winder, M.: Ocean acidification reduces transfer of
658 essential biomolecules in a natural plankton community, *Sci. Rep.*, 6(1), 27749,
659 doi:10.1038/srep27749, 2016.

660 Booth, B. C.: Size classes and major taxonomic groups of phytoplankton at two locations in the
661 subarctic pacific ocean in May and August, 1984, *Mar. Biol.*, 97(2), 275–286,
662 doi:10.1007/BF00391313, 1988.

663 Bopp, L. , Monfray, P. , Aumont, O. , Dufresne, J.-L. , Le Treut, H. , Madec, G. , Terray, L. . and
664 Orr, J. C. .: Potential impact of climate change on marine export production, *Global Biogeochem.*
665 *Cycles*, 15(1), 81–99, doi:10.1029/1999GB001256, 2001.

666 Boras, J. A., Borrull, E., Cardelu, C., Cros, L., Gomes, A., Sala, M. M., Aparicio, F. L., Balague, V.,
667 Mestre, M., Movilla, J., Sarmiento, H., Va, E. and Lo, A.: Contrasting effects of ocean acidification on

668 the microbial food web under different trophic conditions, *ICES J. Mar. Sci.*, 73(73 (3)), 670–679,
669 2016.

670 Boyd, P. W. and Doney, S. C.: Modelling regional responses by marine pelagic ecosystems to
671 global climate change, *Geophys. Res. Lett.*, 29(16), 1–4, 2002.

672 Boyd, P. W., Rynearson, T. A., Armstrong, E. A., Fu, F., Hayashi, K., Hu, Z., Hutchins, D. A., Kudela,
673 R. M., Litchman, E., Mulholland, M. R., Passow, U., Strzepek, R. F., Whittaker, K. A., Yu, E. and
674 Thomas, M. K.: Marine Phytoplankton Temperature versus Growth Responses from Polar to
675 Tropical Waters - Outcome of a Scientific Community-Wide Study, *PLoS One*, 8(5),
676 doi:10.1371/journal.pone.0063091, 2013.

677 Brussaard, C. P. D., Noordeloos, A. A. M., Witte, H., Collenteur, M. C. J., Schulz, K., Ludwig, A. and
678 Riebesell, U.: Arctic microbial community dynamics influenced by elevated CO₂ levels,
679 *Biogeosciences*, 10(2), 719–731, doi:10.5194/bg-10-719-2013, 2013.

680 Calbet, A., Sazhin, A. F., Nejstgaard, J. C., Berger, S. a, Tait, Z. S., Olmos, L., Sousoni, D., Isari, S.,
681 Martínez, R. a, Bouquet, J.-M., Thompson, E. M., Båmstedt, U. and Jakobsen, H. H.: Future climate
682 scenarios for a coastal productive planktonic food web resulting in microplankton phenology
683 changes and decreased trophic transfer efficiency., *PLoS One*, 9(4), e94388,
684 doi:10.1371/journal.pone.0094388, 2014.

685 Chen, S., Beardall, J. and Gao, K.: A red tide alga grown under ocean acidification upregulates its
686 tolerance to lower pH by increasing its photophysiological functions, *Biogeosciences*, 11, 4829–
687 4837, doi:10.5194/bg-11-4829-2014, 2014.

688 Coello-Camba, A. and Agustí, S.: Acidification counteracts negative effects of warming on diatom
689 silicification, *Biogeosciences Discuss.*, 30(October), 1–19, doi:10.5194/bg-2016-424, 2016.

690 Coello-Camba, A., Agustí, S., Holding, J., Arrieta, J. M. and Duarte, C. M.: Interactive effect of
691 temperature and CO₂ increase in Arctic phytoplankton, *Front. Mar. Sci.*,
692 1(October), 1–10, doi:10.3389/fmars.2014.00049, 2014.

693 Delille, B., Harlay, J., Zondervan, I., Jacquet, S., Chou, L., Wollast, R., Bellerby, R. G. J.,
694 Frankignoulle, M., Borges, A. V., Riebesell, U. and Gattuso, J.-P.: Response of primary production
695 and calcification to changes of p CO₂ during experimental blooms of the coccolithophorid
696 *Emiliana huxleyi*, *Global Biogeochem. Cycles*, 19(2), n/a-n/a, doi:10.1029/2004GB002318,
697 2005.

698 Deppeler, S. L. and Davidson, A. T.: Southern Ocean Phytoplankton in a Changing Climate, *Front.*
699 *Mar. Sci.*, 4(February), doi:10.3389/fmars.2017.00040, 2017.

700 Dickson, A. G. and Millero, F. J.: A comparison of the equilibrium constants for the dissociation of
701 carbonic acid in seawater media, *Deep Sea Res. Part I Oceanogr. Res. Pap.*, 34(111), 1733–1743,
702 1987.

703 Dunne, J. P.: A roadmap on ecosystem change, *Nat. Clim. Chang.*, 5, 20 [online] Available from:
704 <http://dx.doi.org/10.1038/nclimate2480>, 2014.

705 Edwards, M., Johns, D., Leterme, S. C., Svendsen, E. and Richardson, A. J.: Regional climate change
706 and harmful algal blooms in the northeast Atlantic, *Limnol. Oceanogr.*, 51(2), 820–829,
707 doi:10.4319/lo.2006.51.2.0820, 2006.

708 Eilertsen, H. and Raa, J.: Toxins in seawater produced by a common phytoplankter : phaeocystis
709 pouchetii, *J. Mar. Biotechnol.*, 3(1), 115–119 [online] Available from:
710 <http://ci.nii.ac.jp/naid/10002209414/en/> (Accessed 28 January 2016), 1995.

711 Engel, A., Schulz, K. G., Riebesell, U., Bellerby, R., Delille, B. and Schartau, M.: Effects of CO₂ on
712 particle size distribution and phytoplankton abundance during a mesocosm bloom experiment
713 (PeECE II), *Biogeosciences*, 5, 509–521, doi:10.5194/bgd-4-4101-2007, 2008.

714 Eppley, R. W.: Temperature and phytoplankton growth in the sea, *Fish. Bull.*, 70(4), 1063–1085,
715 1972.

716 Errera, R. M., Yvon-Lewis, S., Kessler, J. D. and Campbell, L.: Responses of the dinoflagellate
717 *Karenia brevis* to climate change: pCO₂ and sea surface temperatures, *Harmful Algae*, 37, 110–
718 116, doi:10.1016/j.hal.2014.05.012, 2014.

719 Feng, Y., Warner, M. E., Zhang, Y., Sun, J., Fu, F.-X., Rose, J. M. and Hutchins, D. a.: Interactive
720 effects of increased pCO₂, temperature and irradiance on the marine coccolithophore *Emiliana*
721 *huxleyi* (Prymnesiophyceae), *Eur. J. Phycol.*, 43(1), 87–98, doi:10.1080/09670260701664674,
722 2008.

723 Feng, Y., Hare, C., Leblanc, K., Rose, J., Zhang, Y., DiTullio, G., Lee, P., Wilhelm, S., Rowe, J., Sun, J.,
724 Nemcek, N., Gueguen, C., Passow, U., Benner, I., Brown, C. and Hutchins, D.: Effects of increased
725 pCO₂ and temperature on the North Atlantic spring bloom. I. The phytoplankton community
726 and biogeochemical response, *Mar. Ecol. Prog. Ser.*, 388, 13–25, doi:10.3354/meps08133, 2009.

727 Fu, F.-X., Warner, M. E., Zhang, Y., Feng, Y. and Hutchins, D. a.: Effects of Increased Temperature
728 and CO₂ on Photosynthesis, Growth, and Elemental Ratios in Marine *Synechococcus* and
729 *Prochlorococcus* (Cyanobacteria), *J. Phycol.*, 43(3), 485–496, doi:10.1111/j.1529-
730 8817.2007.00355.x, 2007a.

731 Fu, F.-X., Warner, M. E., Zhang, Y., Feng, Y. and Hutchins, D. a.: Effects of Increased Temperature

732 and CO₂ on Photosynthesis, Growth, and Elemental Ratios in Marine *Synechococcus* and
733 *Prochlorococcus* (Cyanobacteria), *J. Phycol.*, 43(3), 485–496, doi:10.1111/j.1529-
734 8817.2007.00355.x, 2007b.

735 Fu, F.-X., Zhang, Y., Warner, M. E., Feng, Y., Sun, J. and Hutchins, D. a.: A comparison of future
736 increased CO₂ and temperature effects on sympatric *Heterosigma akashiwo* and *Prorocentrum*
737 minimum, *Harmful Algae*, 7(1), 76–90, doi:10.1016/j.hal.2007.05.006, 2008.

738 Gao, G., Jin, P., Liu, N., Li, F., Tong, S., Hutchins, D. A. and Gao, K.: The acclimation process of
739 phytoplankton biomass, carbon fixation and respiration to the combined effects of elevated
740 temperature and pCO₂ in the northern South China Sea, *Mar. Pollut. Bull.*, 118(1–2), 213–220,
741 doi:10.1016/j.marpolbul.2017.02.063, 2017.

742 Giordano, M., Beardall, J. and Raven, J. a: CO₂ concentrating mechanisms in algae: mechanisms,
743 environmental modulation, and evolution., *Annu. Rev. Plant Biol.*, 56(January), 99–131,
744 doi:10.1146/annurev.arplant.56.032604.144052, 2005.

745 Goldman, J. and Carpenter, E.: A kinetic approach to the effect of temperature on algal growth,
746 *Limnol. Oceanogr.*, 19(5), 756–766, doi:10.4319/lo.1974.19.5.0756, 1974.

747 Hansen, P.: Effect of high pH on the growth and survival of marine phytoplankton: implications
748 for species succession, *Aquat. Microb. Ecol.*, 28, 279–288, doi:10.3354/ame028279, 2002.

749 Hare, C., Leblanc, K., DiTullio, G., Kudela, R., Zhang, Y., Lee, P., Riseman, S. and Hutchins, D.:
750 Consequences of increased temperature and CO₂ for phytoplankton community structure in the
751 Bering Sea, *Mar. Ecol. Prog. Ser.*, 352, 9–16, doi:10.3354/meps07182, 2007a.

752 Hare, C., Leblanc, K., DiTullio, G., Kudela, R., Zhang, Y., Lee, P., Riseman, S. and Hutchins, D.:
753 Consequences of increased temperature and CO₂ for phytoplankton community structure in the
754 Bering Sea, *Mar. Ecol. Prog. Ser.*, 352, 9–16, doi:10.3354/meps07182, 2007b.

755 Hinga, K. R.: Effects of pH on coastal marine phytoplankton, *Mar. Ecol. Prog. Ser.*, 238, 281–300,
756 2002.

757 Hoogstraten, a., Peters, M., Timmermans, K. R. and De Baar, H. J. W.: Combined effects of
758 inorganic carbon and light on *Phaeocystis globosa* Scherffel (Prymnesiophyceae),
759 *Biogeosciences*, 9(5), 1885–1896, doi:10.5194/bg-9-1885-2012, 2012.

760 Hutchins, D. a., Fu, F.-X., Zhang, Y., Warner, M. E., Feng, Y., Portune, K., Bernhardt, P. W. and
761 Mulholland, M. R.: CO₂ control of *Trichodesmium* N₂ fixation, photosynthesis, growth rates, and
762 elemental ratios: Implications for past, present, and future ocean biogeochemistry, *Limnol.*
763 *Oceanogr.*, 52(4), 1293–1304, doi:10.4319/lo.2007.52.4.1293, 2007.

764 Ipcc: Climate Change 2013: The Physical Science Basis. Contribution of Working Group I to the
765 Fifth Assessment Report of the Intergovernmental Panel on Climate Change, Intergov. Panel
766 Clim. Chang. Work. Gr. I Contrib. to IPCC Fifth Assess. Rep. (AR5)(Cambridge Univ Press. New
767 York), 1535, doi:10.1029/2000JD000115, 2013.

768 Keys, M.: "Effects of future CO₂ and temperature regimes on phytoplankton community
769 composition, biomass and photosynthetic rates in the Western English Channel", PhD thesis.,
770 University of Essex, United Kingdom., 2017.

771 Keys, M., Tilstone, G., Findlay, H. S., Widdicombe, C. E. and Lawson, T.: Effects of elevated CO₂ on
772 phytoplankton community biomass and species composition during a spring *Phaeocystis* spp.
773 bloom in the western English Channel, *Harmful Algae*, 67, 92–106,
774 doi:10.1016/j.hal.2017.06.005, 2017.

775 Kiefer, D. a. and Mitchell, B. G.: A simple steady state description of phytoplankton growth based
776 on absorption cross section and quantum efficiency, *Limnol. Oceanogr.*, 28(4), 770–776,
777 doi:10.4319/lo.1983.28.4.0770, 1983.

778 Kim, J.-M., Lee, K., Shin, K., Kang, J.-H., Lee, H.-W., Kim, M., Jang, P.-G. and Jang, M.-C.: The effect of
779 seawater CO₂ concentration on growth of a natural phytoplankton assemblage in a controlled
780 mesocosm experiment, *Limnol. Oceanogr.*, 51(4), 1629–1636, doi:10.4319/lo.2006.51.4.1629,
781 2006a.

782 Kim, J.-M., Lee, K., Shin, K., Kang, J.-H., Lee, H.-W., Kim, M., Jang, P.-G. and Jang, M.-C.: The effect of
783 seawater CO₂ concentration on growth of a natural phytoplankton assemblage in a controlled
784 mesocosm experiment, *Limnol. Oceanogr.*, 51(4), 1629–1636, doi:10.4319/lo.2006.51.4.1629,
785 2006b.

786 Kitidis, V., Hardman-mountford, N. J., Litt, E., Brown, I., Cummings, D., Hartman, S., Hydes, D.,
787 Fishwick, J. R., Harris, C., Martinez-vicente, V., Woodward, E. M. S. and Smyth, T. J.: Seasonal
788 dynamics of the carbonate system in the Western English Channel, *Cont. Shelf Res.*, 42, 2–12,
789 2012.

790 Kolber, Z. S., Prášil, O. and Falkowski, P. G.: Measurements of variable chlorophyll fluorescence
791 using fast repetition rate techniques: Defining methodology and experimental protocols,
792 *Biochim. Biophys. Acta - Bioenerg.*, 1367(1–3), 88–106, doi:10.1016/S0005-2728(98)00135-2,
793 1998.

794 Lawrenz, E., Silsbe, G., Capuzzo, E., Ylöstalo, P., Forster, R. M., Simis, S. G. H., Prášil, O.,
795 Kromkamp, J. C., Hickman, A. E., Moore, C. M., Forget, M. H., Geider, R. J. and Suggett, D. J.:
796 Predicting the Electron Requirement for Carbon Fixation in Seas and Oceans, *PLoS One*, 8(3),

797 doi:10.1371/journal.pone.0058137, 2013.

798 Laws, E. A., Falkowski, P. G., Smith, W. O., Ducklow, H. W. and McCarthy, J. J.: Temperature effects
799 on export production in the open ocean, *Global Biogeochem. Cycles*, 14(4), 1231–1246,
800 doi:10.1029/1999GB001229, 2000.

801 Li, W. K. W., McLaughlin, F. A., Lovejoy, C. and Carmack, E. C.: Smallest Algae Thrive As the Arctic
802 Ocean Freshens, *Science* (80-.), 326(5952), 539–539, doi:10.1126/science.1179798, 2009.

803 Lomas, M. W. and Glibert, P. M.: Interactions between NH₄⁺ and NO₃⁻ uptake and
804 assimilation: Comparison of diatoms and dinoflagellates at several growth temperatures, *Mar.*
805 *Biol.*, 133(3), 541–551, doi:10.1007/s002270050494, 1999.

806 Love, B. A., Olson, M. B. and Wuori, T.: Technical Note: A minimally-invasive experimental
807 system for pCO₂ manipulation in plankton cultures
808 using passive gas exchange (Atmospheric Carbon Control Simulator), *Biogeosciences Discuss.*,
809 (December), 1–19, doi:10.5194/bg-2016-502, 2016.

810 Matear, R. J. and Lenton, A.: Carbon–climate feedbacks accelerate ocean acidification,
811 *Biogeosciences*, 15(6), 1721–1732, doi:10.5194/bg-15-1721-2018, 2018.

812 Maugendre, L., Gattuso, J. P., Poulton, A. J., Dellisanti, W., Gaubert, M., Guieu, C. and Gazeau, F.: No
813 detectable effect of ocean acidification on plankton metabolism in the NW oligotrophic
814 Mediterranean Sea: Results from two mesocosm studies, *Estuar. Coast. Shelf Sci.*, 186, 89–99,
815 doi:10.1016/j.ecss.2015.03.009, 2017.

816 Mehrbach, C., Culbertson, C. H., Hawley, J. E. and Pytkowicz, R. M.: Measurement of the Apparent
817 Dissociation Constants of Carbonic Acid in Seawater at Atmospheric Pressure, *Limnol.*
818 *Oceanogr.*, 18(1932), 897–907, 1973.

819 Menden-Deuer, S. and Lessard, E. J.: Carbon to volume relationships for dinoflagellates, diatoms,
820 and other protist plankton, *Limnol. Oceanogr.*, 45(3), 569–579, doi:10.4319/lo.2000.45.3.0569,
821 2000.

822 Morán, X. A. G., López-Urrutia, Á., Calvo-Díaz, A. and Li, W. K. W.: Increasing importance of small
823 phytoplankton in a warmer ocean, *Glob. Chang. Biol.*, 16(3), 1137–1144, doi:10.1111/j.1365-
824 2486.2009.01960.x, 2010.

825 Morse, D., Salois, P., Markovic, P. and Hastings, J. W.: A nuclear-encoded form II RuBisCO in
826 dinoflagellates., *Science*, 268(5217), 1622–1624, doi:10.1126/science.7777861, 1995.

827 Moustaka-Gouni, M., Kormas, K. A., Scotti, M., Vardaka, E. and Sommer, U.: Warming and

828 Acidification Effects on Planktonic Heterotrophic Pico- and Nanoflagellates in a Mesocosm
829 Experiment, *Protist*, 167(4), 389–410, doi:10.1016/j.protis.2016.06.004, 2016.

830 Oxborough, K., Moore, C. M., Suggett, D. J., Lawson, T., Chan, H. G. and Geider, R. J.: Direct
831 estimation of functional PSII reaction center concentration and PSII electron flux on a volume
832 basis: a new approach to the analysis of Fast Repetition Rate fluorometry (FRRf) data, *Limnol.*
833 *Oceanogr. Methods*, 10, 142–154, doi:10.4319/lom.2012.10.142, 2012.

834 Paul, C., Matthiessen, B. and Sommer, U.: Warming, but not enhanced CO₂ concentration,
835 quantitatively and qualitatively affects phytoplankton biomass, *Mar. Ecol. Prog. Ser.*, 528, 39–51,
836 doi:10.3354/meps11264, 2015.

837 Paulino, a. I., Egge, J. K. and Larsen, a.: Effects of increased atmospheric CO₂ on small and
838 intermediate sized osmotrophs during a nutrient induced phytoplankton bloom, *Biogeosciences*
839 *Discuss.*, 4(6), 4173–4195, doi:10.5194/bgd-4-4173-2007, 2007.

840 Peter, K. H. and Sommer, U.: Phytoplankton Cell Size: Intra- and Interspecific Effects of
841 Warming and Grazing, *PLoS One*, 7(11), doi:10.1371/journal.pone.0049632, 2012.

842 Pierrot, D., Lewis, E. and Wallace, D. W. R.: MS Excel program developed for CO₂ system
843 calculations, ORNL/CDIAC-105a. Carbon Dioxide Inf. Anal. Center, Oak Ridge Natl. Lab. US Dep.
844 Energy, Oak Ridge, Tennessee, 2006.

845 Raupach, M. R., Marland, G., Ciais, P., Le Quéré, C., Canadell, J. G., Klepper, G. and Field, C. B.:
846 Global and regional drivers of accelerating CO₂ emissions., *Proc. Natl. Acad. Sci. U. S. A.*, 104(24),
847 10288–93, doi:10.1073/pnas.0700609104, 2007.

848 Raven, J., Caldeira, K., Elderfield, H., H.-G. and others: Ocean acidification due to increasing
849 atmospheric carbon dioxide, *R. Soc.*, (June), 2005.

850 Raven, J. A. and Geider, R. J.: Temperature and algal growth, *New Phytol.*, 110(4), 441–461,
851 doi:10.1111/j.1469-8137.1988.tb00282.x, 1988.

852 Reinfelder, J. R.: Carbon Concentrating Mechanisms in Eukaryotic Marine Phytoplankton, *Ann.*
853 *Rev. Mar. Sci.*, 3(1), 291–315, doi:10.1146/annurev-marine-120709-142720, 2011.

854 Riebesell, U.: Effects of CO₂ Enrichment on Marine Phytoplankton, *J. Oceanogr.*, 60(4), 719–729,
855 doi:10.1007/s10872-004-5764-z, 2004.

856 Riebesell, U., Schulz, K. G., Bellerby, R. G. J., Botros, M., Fritsche, P., Meyerhöfer, M., Neill, C.,
857 Nondal, G., Oschlies, a, Wohlers, J. and Zöllner, E.: Enhanced biological carbon consumption in a
858 high CO₂ ocean., *Nature*, 450(7169), 545–8, doi:10.1038/nature06267, 2007.

859 Riebesell, U., Fabry, V. J., Hansson, L. and Gattuso, J.-P.: Guide to best practices for ocean
860 acidification, edited by L. H. and J. -P. G. L. U. Riebesell, V. J. Fabry, Publications Office Of The
861 European Union., 2010.

862 Rost, B., Riebesell, U., Burkhardt, S. and Su, D.: Carbon acquisition of bloom-forming marine
863 phytoplankton, *Limnol. Oceanogr.*, 48(1), 55–67, 2003.

864 Sathyendranath, S., Stuart, V., Nair, A., Oka, K., Nakane, T., Bouman, H., Forget, M. H., Maass, H.
865 and Platt, T.: Carbon-to-chlorophyll ratio and growth rate of phytoplankton in the sea, *Mar. Ecol.*
866 *Prog. Ser.*, 383, 73–84, doi:10.3354/meps07998, 2009.

867 Savage, V. M., Gillooly, J. F., Brown, J. H., West, G. B. and Charnov, E. L.: Effects of Body Size and
868 Temperature on Population Growth, *Am. Nat.*, 163(3), 429–441, doi:10.1086/381872, 2004.

869 Schoemann, V., Becquevort, S., Stefels, J., Rousseau, V. and Lancelot, C.: Phaeocystis blooms in the
870 global ocean and their controlling mechanisms: a review, *J. Sea Res.*, 53(1–2), 43–66,
871 doi:10.1016/j.seares.2004.01.008, 2005.

872 Schulz, K. G., Ramos, J. B., Zeebe, R. E. and Riebesell, U.: Biogeosciences CO₂ perturbation
873 experiments : similarities and differences between dissolved inorganic carbon and total
874 alkalinity manipulations, *Biogeosciences*, 6, 2145–2153, 2009.

875 Shi, D., Xu, Y. and Morel, F. M. M.: Effects of the pH/pCO₂ control method on medium chemistry
876 and phytoplankton growth, *Biogeosciences*, 6(7), 1199–1207, doi:10.5194/bg-6-1199-2009,
877 2009.

878 Smetacek, V. and Cloern, J. E.: On Phytoplankton Trends, *Science (80-.)*, 319(5868), 1346–1348
879 [online] Available from: <http://www.jstor.org/stable/20053523>, 2008.

880 Smyth, T. J., Fishwick, J. R., AL-Moosawi, L., Cummings, D. G., Harris, C., Kitidis, V., Rees, A.,
881 Martinez-Vicente, V. and Woodward, E. M. S.: A broad spatio-temporal view of the Western
882 English Channel observatory, *J. Plankton Res.*, 32(5), 585–601, doi:10.1093/plankt/fbp128,
883 2010.

884 Strom, S.: Novel interactions between phytoplankton and microzooplankton : their influence on
885 the coupling between growth and grazing rates in the sea, , 41–54, 2002.

886 Tarran, G. a., Heywood, J. L. and Zubkov, M. V.: Latitudinal changes in the standing stocks of
887 nano- and picoeukaryotic phytoplankton in the Atlantic Ocean, *Deep Sea Res. Part II Top. Stud.*
888 *Oceanogr.*, 53(14–16), 1516–1529, doi:10.1016/j.dsr2.2006.05.004, 2006.

889 Taucher, J., Jones, J., James, A., Brzezinski, M. A., Carlson, C. A., Riebesell, U. and Passow, U.:

890 Combined effects of CO₂ and temperature on carbon uptake and partitioning by the marine
891 diatoms *Thalassiosira weissflogii* and *Dactyliosolen fragilissimus*, *Limnol. Oceanogr.*, 60(3),
892 901–919, doi:10.1002/lno.10063, 2015.

893 Thoisen, C., Riisgaard, K., Lundholm, N., Nielsen, T. and Hansen, P.: Effect of acidification on an
894 Arctic phytoplankton community from Disko Bay, West Greenland, *Mar. Ecol. Prog. Ser.*, 520,
895 21–34, doi:10.3354/meps11123, 2015.

896 Thomas, M. K., Kremer, C. T., Klausmeier, C. A. and Litchman, E.: A Global Pattern of Thermal
897 Adaptation in Marine Phytoplankton, *Science* (80-.), 338(6110), 1085–1088,
898 doi:10.1126/science.1224836, 2012.

899 Torstensson, A., Chierici, M. and Wulff, A.: The influence of increased temperature and carbon
900 dioxide levels on the benthic/sea ice diatom *Navicula directa*, *Polar Biol.*, 35(2), 205–214,
901 doi:10.1007/s00300-011-1056-4, 2012.

902 Tortell, P., DiTullio, G., Sigman, D. and Morel, F.: CO₂ effects on taxonomic composition and
903 nutrient utilization in an Equatorial Pacific phytoplankton assemblage, *Mar. Ecol. Prog. Ser.*, 236,
904 37–43, doi:10.3354/meps236037, 2002.

905 Tortell, P. D., Payne, C. D., Li, Y., Trimborn, S., Rost, B., Smith, W. O., Riesselman, C., Dunbar, R. B.,
906 Sedwick, P. and DiTullio, G. R.: CO₂ sensitivity of Southern Ocean phytoplankton, *Geophys. Res.*
907 *Let.*, 35(4), L04605, doi:10.1029/2007GL032583, 2008.

908 Utermöhl, H.: Zur vervollkommnung der quantitativen phytoplankton-methodik, *Mitt. int. Ver.*
909 *theor. angew. Limnol.*, 9, 1–38, 1958.

910 Verity, P. G., Brussaard, C. P., Nejtgaard, J. C., Van Leeuwe, M. a., Lancelot, C. and Medlin, L. K.:
911 Current understanding of *Phaeocystis* ecology and biogeochemistry, and perspectives for future
912 research, edited by M. A. van Leeuwe, J. Stefels, S. Belviso, C. Lancelot, P. G. Verity, and W. W. C.
913 Gieskes, Springer Netherlands., 2007.

914 Webb, W. L., Newton, M. and Starr, D.: Carbon dioxide exchange of *Alnus rubra*, *Oecologia*, 17(4),
915 281–291, doi:10.1007/BF00345747, 1974.

916 Welschmeyer: Fluorometric analysis of chlorophyll a in the presence of chlorophyll b and
917 pheopigments, *Limnol. Oceanogr.*, 39(8), 1985–1992, 1994.

918 Widdicombe, C. E., Eloire, D., Harbour, D., Harris, R. P. and Somerfield, P. J.: Long-term
919 phytoplankton community dynamics in the Western English Channel, *J. Plankton Res.*, 32(5),
920 643–655, doi:10.1093/plankt/fbp127, 2010a.

921 Widdicombe, C. E., Eloire, D., Harbour, D., Harris, R. P. and Somerfield, P. J.: Long-term
922 phytoplankton community dynamics in the Western English Channel, *J. Plankton Res.*, 32(5),
923 643–655, doi:10.1093/plankt/fbp127, 2010b.

924 Wolf-gladrow, B. D. A., Riebesell, U. L. F., Burkhardt, S. and Jelle, B.: Direct effects of CO₂
925 concentration on growth and isotopic composition of marine plankton, *Tellus*, 51B, 461–476,
926 1999.

927 Woods, H. A. and Harrison, J. F.: Temperature and the chemical composition of poikilothermic
928 organisms, , (Sidell 1998), 237–245, 2003.

929

930

931

932

933

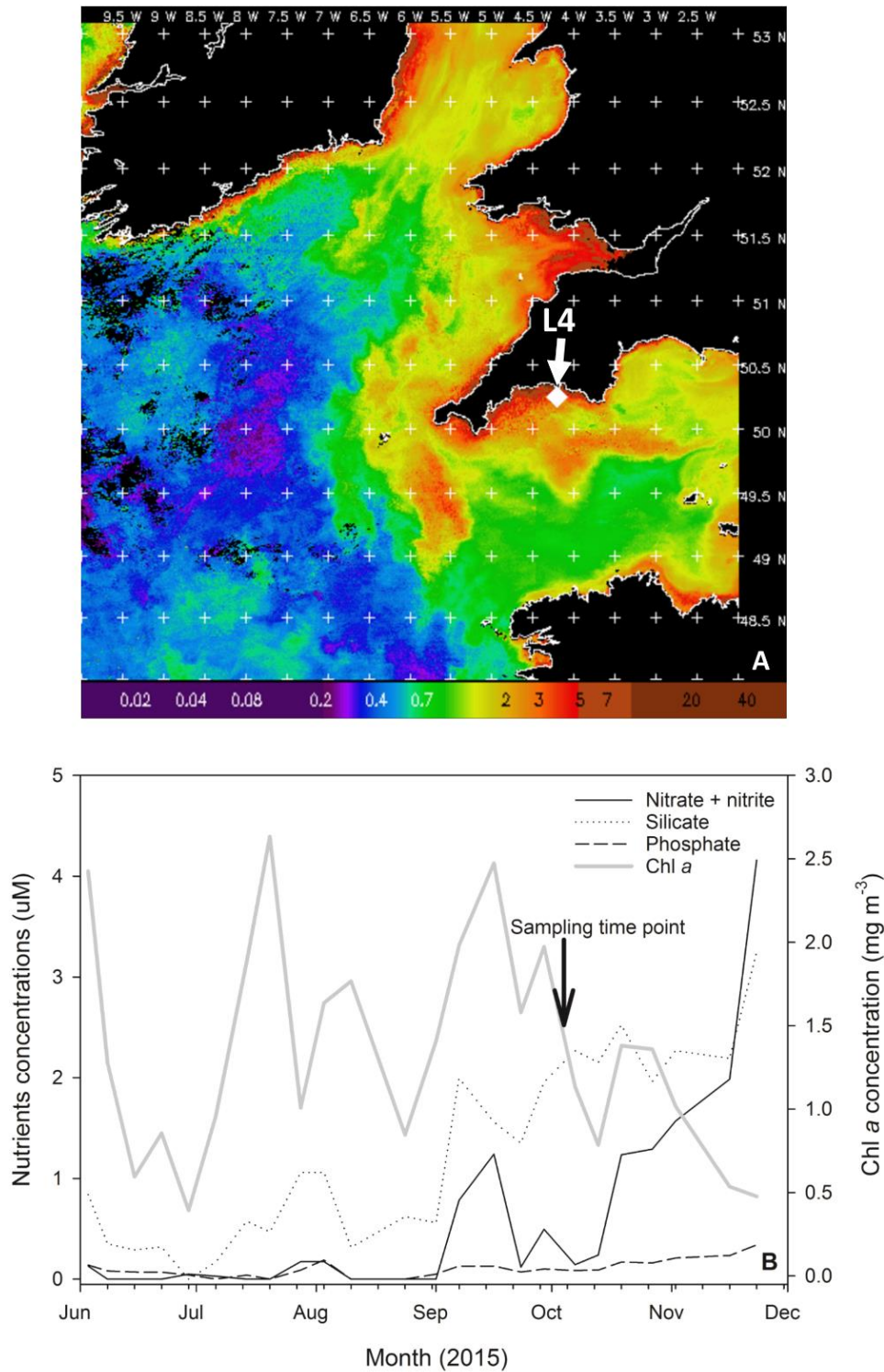


Fig. 1. (A). MODIS weekly composite chl *a* image of the western English Channel covering the period 30th September – 6th October 2015 (coincident with the week of phytoplankton community sampling for the present study), processing courtesy of NEODAAS. The position of coastal station L4 is marked with a white diamond. (B). Profiles of weekly nutrient and chl *a* concentrations from station L4 at a depth of 10 m over the second half of 2015 in the months prior to phytoplankton community sampling (indicated by black arrow and text).

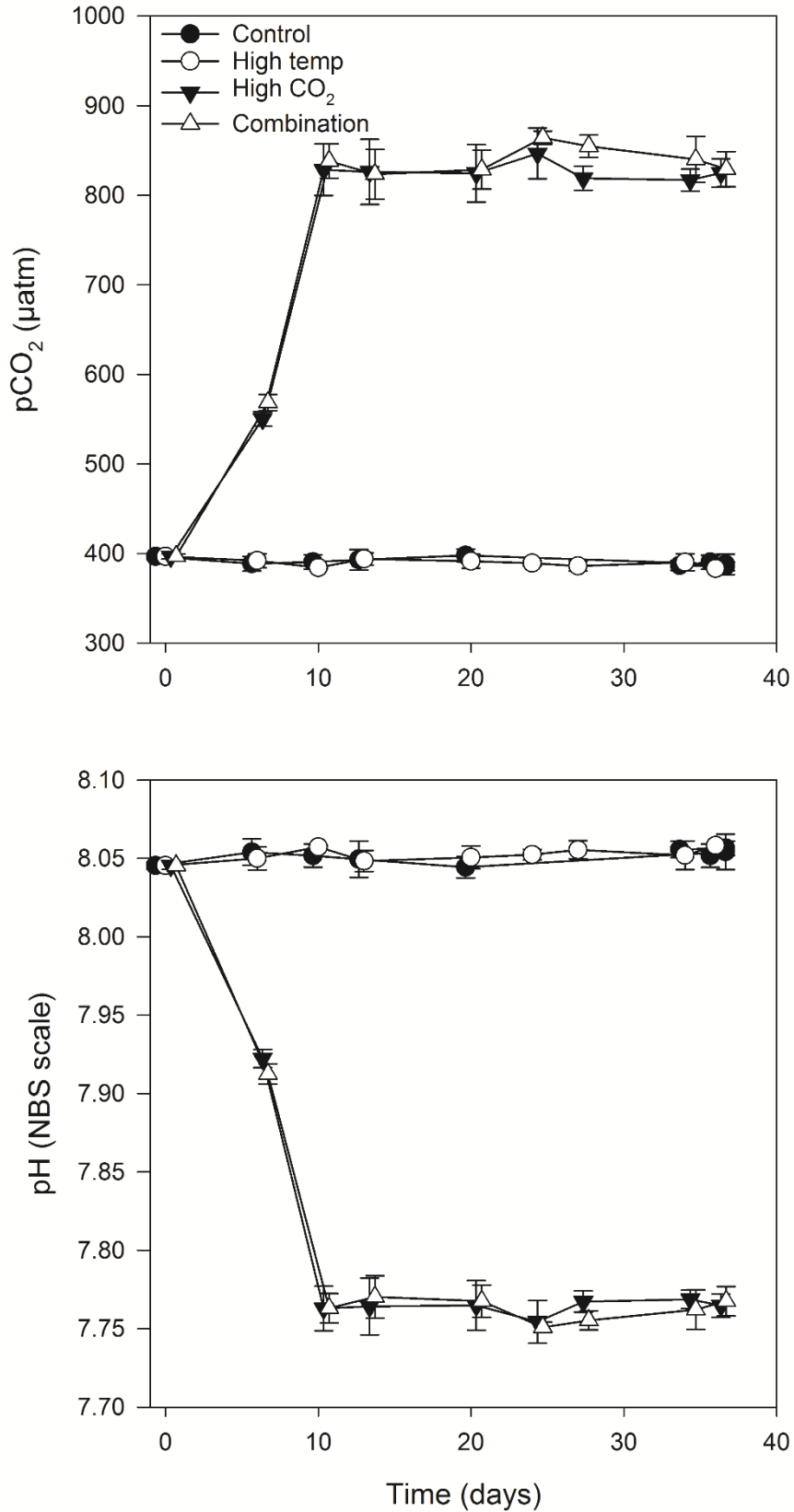


Fig. 2. Calculated values of partial pressure of CO₂ in seawater (pCO₂) (A) and pH (B) from direct measurements of total alkalinity and dissolved inorganic carbon. (For full carbonate system values see **Table S1.**, supplementary material)

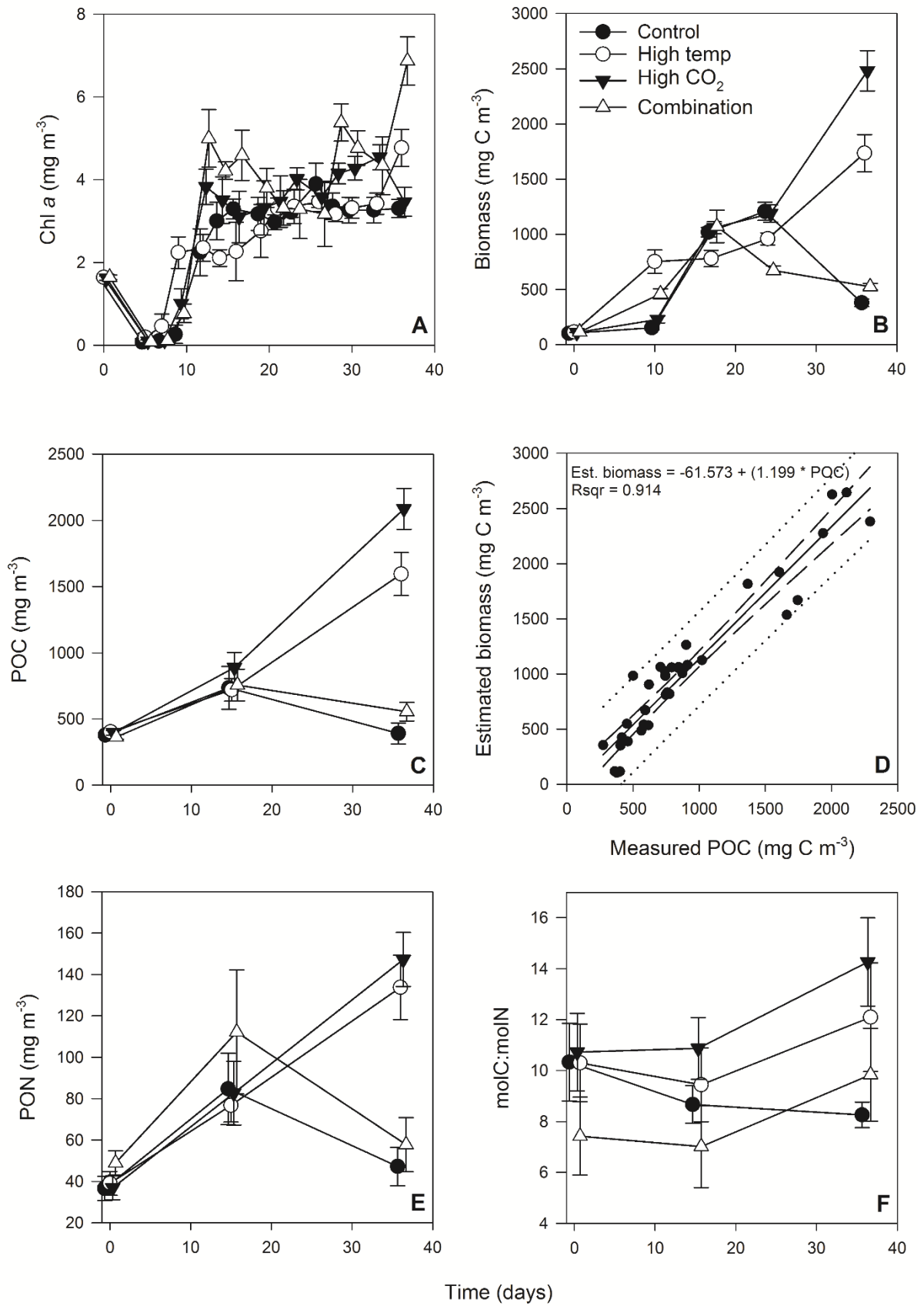


Fig. 3. Time course of chl a (A), estimated phytoplankton biomass (B), POC (C), regression of estimated phytoplankton carbon vs measured POC (D), PON (E) and POC:PON (F).

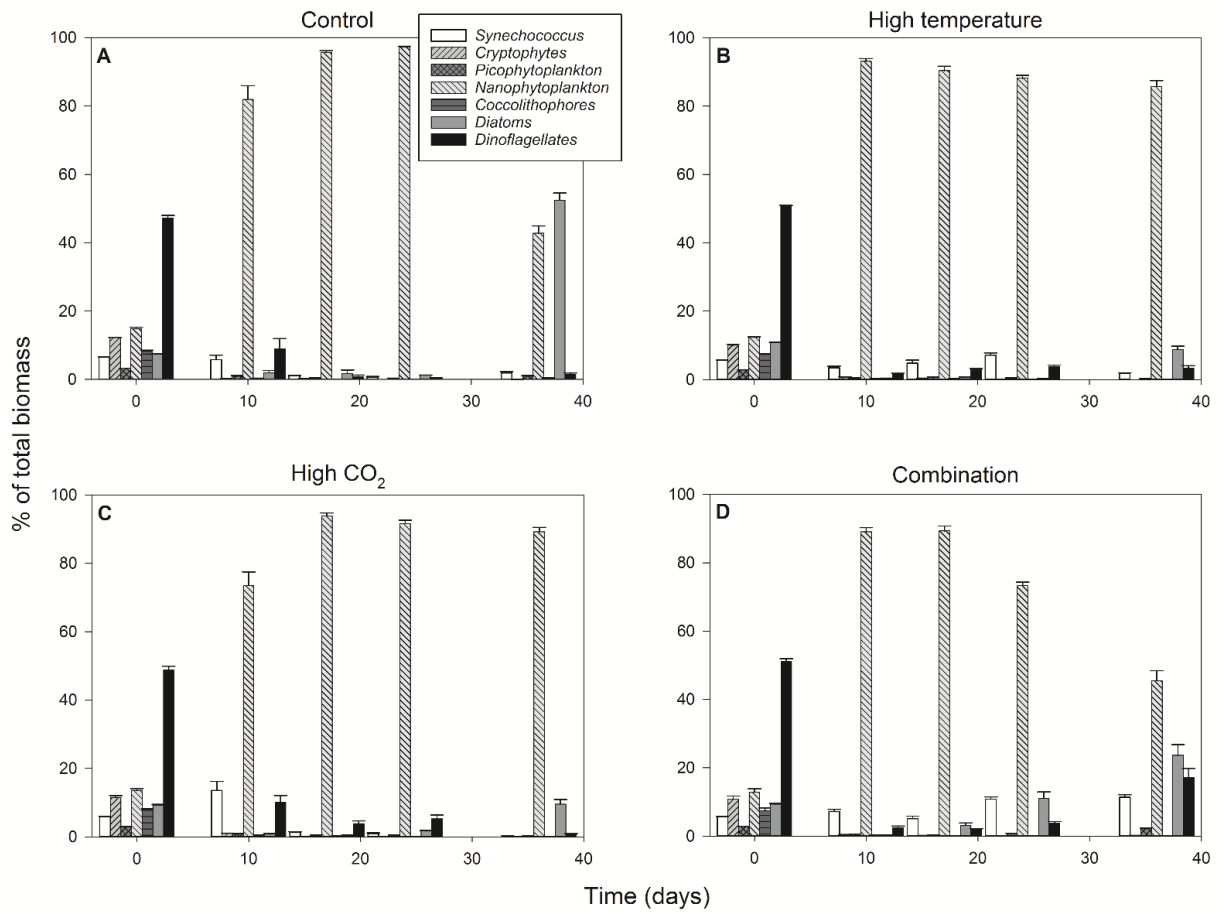


Fig. 4. Percentage contribution to community biomass by phytoplankton groups/species throughout the experiment in the control (A), high temperature (B), high CO₂ (C) and combination treatments (D).

937

938

939

940

941

942

943

944

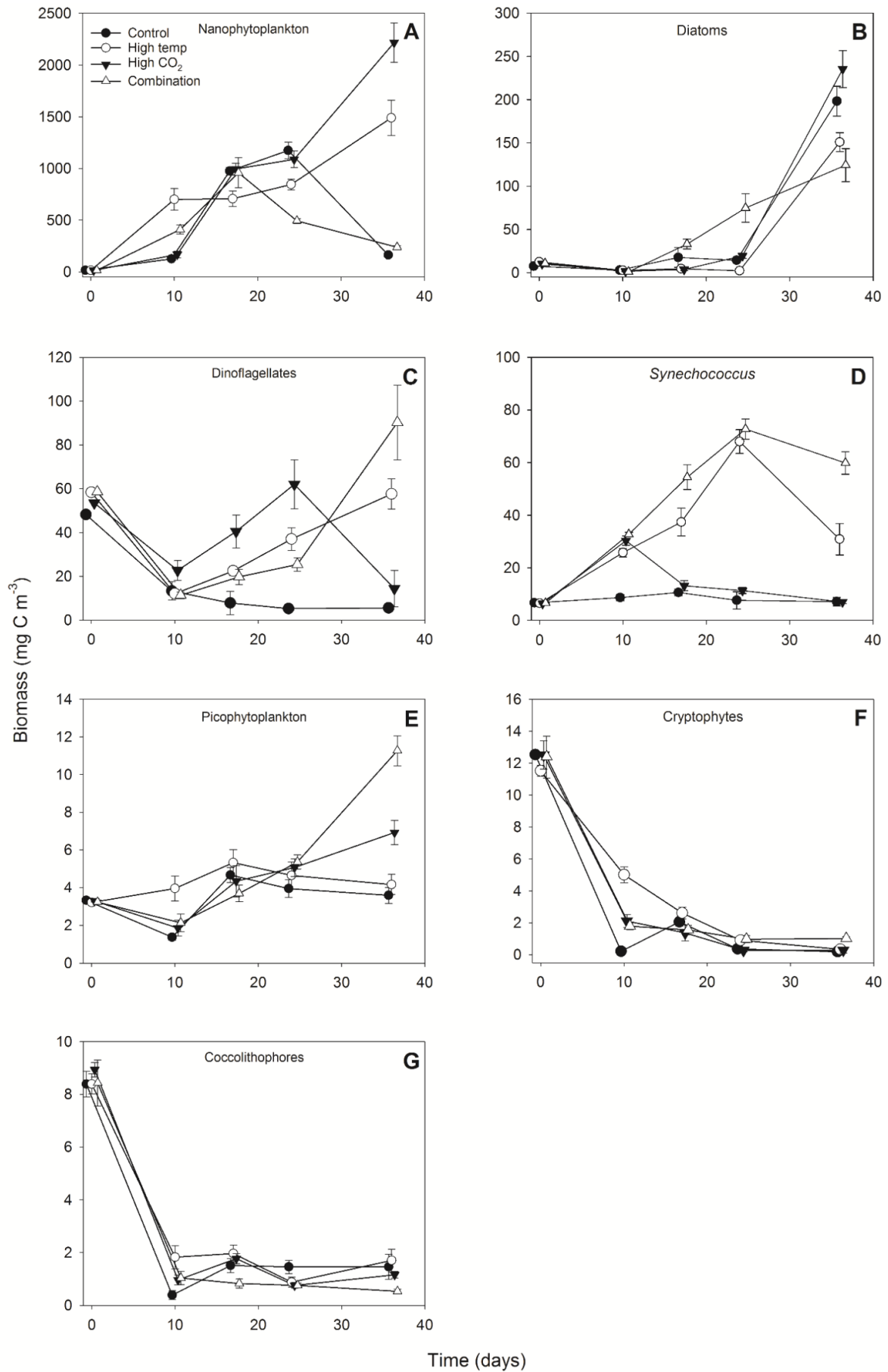


Fig. 5. Response of individual phytoplankton groups to experimental treatments.

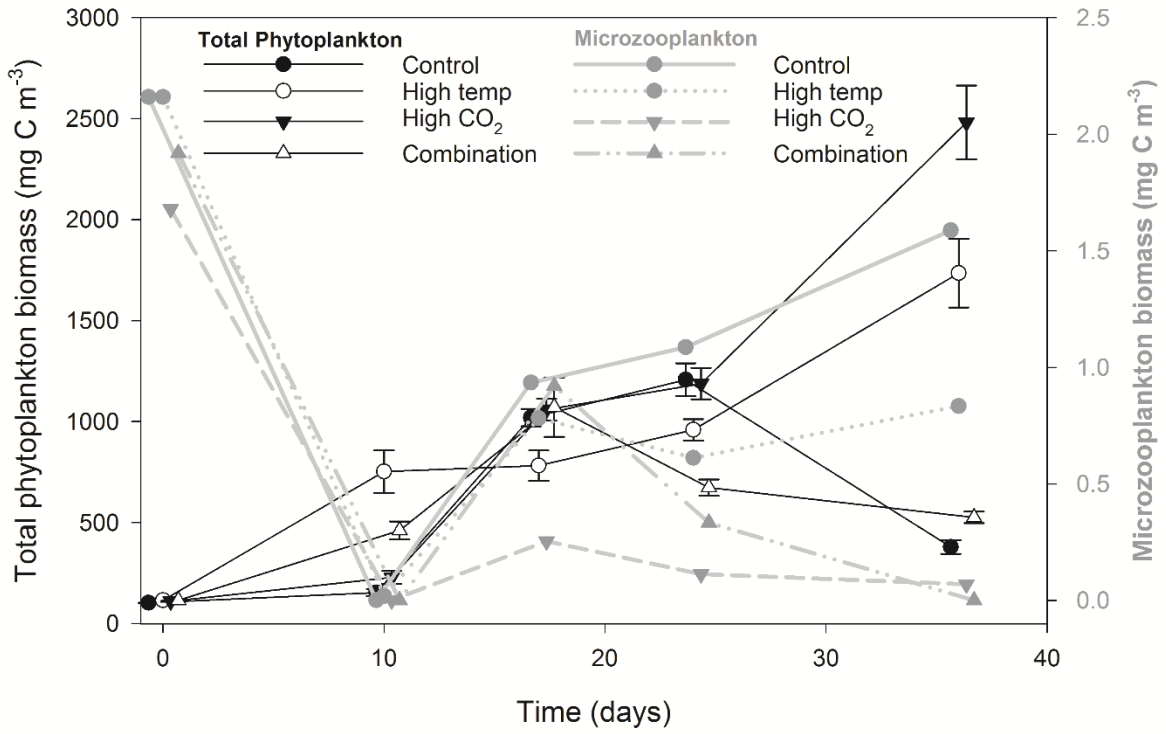


Fig. 6. Microzooplankton biomass (dominated by *Strombolidium* sp.) relative to total phytoplankton biomass.

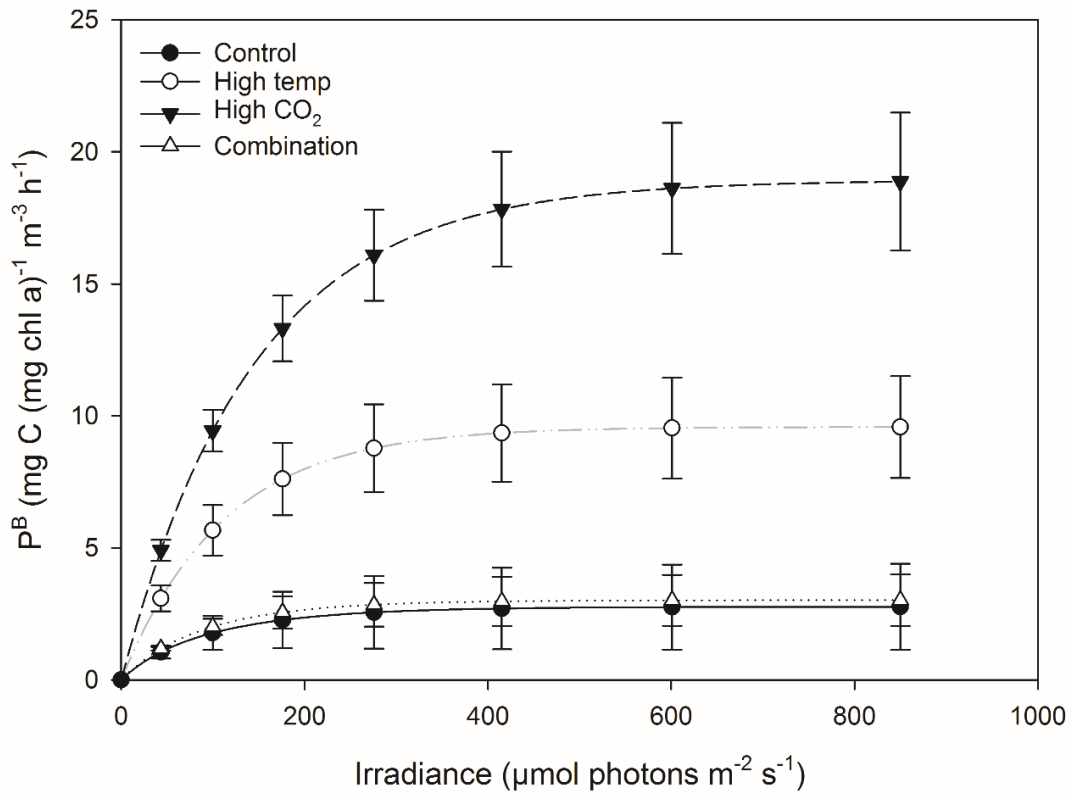


Fig. 7. Fitted parameters of FRRf-based photosynthesis-irradiance curves for the experimental treatments on the final experimental day (T36)

945
946
947

Table 1. Results of generalized linear mixed model testing for effects of time, temperature, pCO₂ and all interactions on chl *a*, phytoplankton biomass and particulate organic carbon and nitrogen. Significant results are in bold; * p < 0.05, ** p < 0.01, *** p < 0.001.

| <u>Response variable</u> | <u>n</u> | <u>df</u> | <u>z-value</u> | <u>p</u> | <u>sig</u> |
|---|----------|-----------|----------------|------------------|------------|
| <u>Chla (mg m⁻³)</u> | | | | | |
| High temp | 516 | 507 | 0.412 | 0.680 | |
| High pCO ₂ | 516 | 507 | 0.664 | 0.507 | |
| Time | 516 | 507 | 3.815 | <0.001 | *** |
| High temp x high pCO ₂ | 516 | 507 | 1.100 | 0.271 | |
| Time x high temp | 516 | 507 | -0.213 | 0.831 | |
| Time x high CO ₂ | 516 | 507 | -0.011 | 0.991 | |
| Time x high temp x high CO ₂ | 516 | 507 | 0.340 | 0.734 | |
| <u>Estimated biomass (mg C m⁻³)</u> | | | | | |
| High temp | 80 | 71 | 0.092 | 0.927 | |
| High pCO ₂ | 80 | 71 | 2.102 | 0.036 | * |
| Time | 80 | 71 | 2.524 | 0.012 | * |
| High temp x high pCO ₂ | 80 | 71 | 1.253 | 0.210 | |
| Time x high temp | 80 | 71 | 1.866 | 0.062 | |
| Time x high CO ₂ | 80 | 71 | 4.414 | <0.001 | *** |
| Time x high temp x high CO ₂ | 80 | 71 | -1.050 | 0.294 | |
| <u>POC (mg m⁻³)</u> | | | | | |
| High temp | 48 | 38 | -0.977 | 0.328 | |
| High pCO ₂ | 48 | 38 | -0.866 | 0.386 | |
| Time | 48 | 38 | -0.203 | 0.839 | |
| High temp x high pCO ₂ | 48 | 38 | -0.29 | 0.772 | |
| Time x high temp | 48 | 38 | 3.648 | <0.001 | *** |
| Time x high CO ₂ | 48 | 38 | 4.333 | <0.001 | *** |
| Time x high temp x high CO ₂ | 48 | 38 | 0.913 | 0.361 | |
| <u>PON (mg m⁻³)</u> | | | | | |
| High temp | 48 | 38 | -0.640 | 0.522 | |
| High pCO ₂ | 48 | 38 | -0.479 | 0.632 | |
| Time | 48 | 38 | 0.202 | 0.84 | |
| High temp x high pCO ₂ | 48 | 38 | 0.667 | 0.505 | |
| Time x high temp | 48 | 38 | 1.674 | 0.094 | |
| Time x high CO ₂ | 48 | 38 | 2.037 | < 0.05 | * |
| Time x high temp x high CO ₂ | 48 | 38 | -0.141 | 0.730 | |
| <u>POC:PON molC:mol N</u> | | | | | |
| High temp | 48 | 38 | 0.222 | 0.824 | |
| High pCO ₂ | 48 | 38 | 0.029 | 0.977 | |
| Time | 48 | 38 | 0.184 | 0.854 | |
| High temp x high pCO ₂ | 48 | 38 | 0.990 | 0.322 | |
| Time x high temp | 48 | 38 | 2.377 | 0.017 | * |
| Time x high CO ₂ | 48 | 38 | 2.748 | 0.005 | ** |
| Time x high temp x high CO ₂ | 48 | 38 | -0.215 | 0.829 | |

948

949
950
951

Table 2. Results of generalized linear mixed model testing for significant effects of time, temperature, pCO₂ and all interactions on phytoplankton species biomass. Significant results are in bold;

* p < 0.05, ** p < 0.01, *** p < 0.001.

| Response variable | n | df | z-value | p | sig |
|---|----------|-----------|----------------|------------------|------------|
| Diatoms (mg C m⁻³) | | | | | |
| High temp | 80 | 70 | -0.216 | 0.829 | |
| High pCO ₂ | 80 | 70 | -0.895 | 0.371 | |
| Time | 80 | 70 | 2.951 | 0.003 | ** |
| High temp x high pCO ₂ | 80 | 70 | 1.063 | 0.288 | |
| Time x high temp | 80 | 70 | -1.151 | 0.250 | |
| Time x high CO ₂ | 80 | 70 | 0.560 | 0.576 | |
| Time x high temp x high CO ₂ | 80 | 70 | 0.368 | 0.713 | |
| Dinoflagellates (mg C m⁻³) | | | | | |
| High temp | 80 | 70 | -0.018 | 0.986 | |
| High pCO ₂ | 80 | 70 | 0.487 | 0.627 | |
| Time | 80 | 70 | -2.347 | 0.019 | * |
| High temp x high pCO ₂ | 80 | 70 | -0.166 | 0.868 | |
| Time x high temp | 80 | 70 | 1.857 | 0.063 | |
| Time x high CO ₂ | 80 | 70 | 1.009 | 0.313 | |
| Time x high temp x high CO ₂ | 80 | 70 | 2.207 | 0.027 | * |
| Nanophytoplankton (mg m⁻³) | | | | | |
| High temp | 80 | 70 | -0.371 | 0.710 | |
| High pCO ₂ | 80 | 70 | -2.108 | 0.035 | * |
| Time | 80 | 70 | 2.162 | 0.031 | * |
| High temp x high pCO ₂ | 80 | 70 | 0.79 | 0.430 | |
| Time x high temp | 80 | 70 | 1.695 | 0.090 | |
| Time x high CO ₂ | 80 | 70 | 3.563 | <0.001 | *** |
| Time x high temp x high CO ₂ | 80 | 70 | -0.806 | 0.420 | |
| Synechococcus (mg m⁻³) | | | | | |
| High temp | 80 | 70 | 3.333 | <0.001 | *** |
| High pCO ₂ | 80 | 70 | 2.231 | 0.026 | * |
| Time | 80 | 70 | 0.049 | 0.961 | |
| High temp x high pCO ₂ | 80 | 70 | 2.391 | 0.017 | * |
| Time x high temp | 80 | 70 | 4.076 | <0.001 | *** |
| Time x high CO ₂ | 80 | 70 | -1.553 | 0.1204 | |
| Time x high temp x high CO ₂ | 80 | 70 | 5.382 | <0.001 | *** |
| Picophytoplankton (mg m⁻³) | | | | | |
| High temp | 80 | 70 | 0.951 | 0.342 | |
| High pCO ₂ | 80 | 70 | -0.472 | 0.637 | |
| Time | 80 | 70 | 0.897 | 0.370 | |
| High temp x high pCO ₂ | 80 | 70 | -1.188 | 0.235 | |
| Time x high temp | 80 | 70 | -0.219 | 0.827 | |
| Time x high CO ₂ | 80 | 70 | 1.411 | 0.158 | |
| Time x high temp x high CO ₂ | 80 | 70 | 2.792 | 0.005 | ** |
| Coccolithophores (mg C m⁻³) | | | | | |
| High temp | 80 | 70 | -0.408 | 0.683 | |
| High pCO ₂ | 80 | 70 | -0.308 | 0.758 | |
| Time | 80 | 70 | 0.211 | 0.833 | |
| High temp x high pCO ₂ | 80 | 70 | -0.319 | 0.750 | |

Table 2 cont'd

| | | | | | |
|---|----|----|--------|------------------|------------|
| Time x high temp | 80 | 70 | 0.269 | 0.788 | |
| Time x high CO ₂ | 80 | 70 | 0.295 | 0.768 | |
| Time x high temp x high CO ₂ | 80 | 70 | 0.502 | 0.615 | |
| Cryptophytes (mg C m⁻³) | | | | | |
| High temp | 80 | 70 | 0.207 | 0.836 | |
| High pCO ₂ | 80 | 70 | 0.256 | 0.798 | |
| Time | 80 | 70 | -5.289 | <0.001 | *** |
| High temp x high pCO ₂ | 80 | 70 | -0.349 | 0.727 | |
| Time x high temp | 80 | 70 | 1.885 | 0.059 | |
| Time x high CO ₂ | 80 | 70 | 0.167 | 0.867 | |
| Time x high temp x high CO ₂ | 80 | 70 | 1.694 | 0.090 | |
| Microzooplankton (mg C m⁻³) | | | | | |
| High temp | 80 | 70 | 0.138 | 0.890 | |
| High pCO ₂ | 80 | 70 | -0.142 | 0.887 | |
| Time | 80 | 70 | 0.418 | 0.676 | |
| High temp x high pCO ₂ | 80 | 70 | 0.314 | 0.753 | |
| Time x high temp | 80 | 70 | -0.930 | 0.352 | |
| Time x high CO ₂ | 80 | 70 | -2.100 | 0.036 | * |
| Time x high temp x high CO ₂ | 80 | 70 | -1.996 | 0.046 | * |

952

953

954

955

956

957

958

959

960

Table 3. FRRf-based photosynthesis-irradiance curve parameters for the experimental treatments on the final day (T36).

| Parameter | Control | sd | High temp | sd | High CO ₂ | sd | Combination | sd |
|----------------------------------|---------|-------|-----------|------|----------------------|-------|-------------|-------|
| P^B_m | 2.77 | 1.63 | 9.58 | 1.94 | 18.93 | 2.65 | 3.02 | 0.97 |
| α | 0.03 | 0.01 | 0.09 | 0.01 | 0.13 | 0.01 | 0.04 | 0.00 |
| I_k | 85.33 | 45.47 | 110.93 | 6.09 | 144.13 | 17.91 | 86.38 | 33.06 |

961

962

963

964

965

966

967

968 **Table 4.** Results of generalised linear model testing for significant effects of temperature, CO₂ and temperature
 969 x CO₂ on phytoplankton photophysiology at T36; P^B_m (maximum photosynthetic rates), α (light limited slope)
 970 and I_k (light saturated photosynthesis). Significant results are in bold; * p < 0.05, ** p < 0.001, *** p < 0.0001.

| Response variable | n | df | t-value | p | sig |
|---|----------|-----------|----------------|-----------------|------------|
| <u>P^B_m</u> | | | | | |
| High temp | 12 | 8 | 7.353 | < 0.0001 | *** |
| High pCO ₂ | 12 | 8 | 8.735 | < 0.0001 | *** |
| High temp x high pCO ₂ | 12 | 8 | -8.519 | < 0.0001 | *** |
| <u>α</u> | | | | | |
| High temp | 12 | 8 | 13.03 | < 0.0001 | *** |
| High pCO ₂ | 12 | 8 | 15.15 | < 0.0001 | *** |
| High temp x high pCO ₂ | 12 | 8 | -14.82 | < 0.0001 | *** |
| <u>I_k</u> | | | | | |
| High temp | 12 | 8 | 2.018 | 0.0783 | |
| High pCO ₂ | 12 | 8 | 2.541 | 0.0347 | * |
| High temp x high pCO ₂ | 12 | 8 | -2.441 | 0.0405 | * |

971

972

973